Research Square

Preprints are preliminary reports that have not undergone peer review.
They should not be considered conclusive, used to inform clinical practice,
or referenced by the media as validated information.

Maternal Gut Microbiota Transplantation Undermined the Lipid and Glucose Metabolism of Newborns in a Piglet Model

Hua Zhou
Animal Nutrition Institute
Jing Sun
Chongqing Academy of Animal Science
Zuohua Liu
Chongqing Academy of Animal Science
Hong Chen
College of Food Science
Liangpeng Ge
Chongqing Academy of Animal Science
Bing Yu
Animal Nutrition Institute
Daiwen Chen (dwchen@sicau.edu.cn)
Sichuan Agricultural University https://orcid.org/0000-0002-8351-7421

Research

Keywords: maternal microbiota transplantation, lipid metabolism, glucose metabolism, piglet model

Posted Date: November 18th, 2020

DOI: https://doi.org/10.21203/rs.3.rs-104735/v1

License: This work is licensed under a Creative Commons Attribution 4.0 International License.
Read Full License

Abstract

Background

The present study was conducted to explore the maternal gut microbiota transplantation on the lipid and glucose metabolism of newborns in a piglet model. Six hysterectomy-derived germ-free (GF) Bama piglets were reared in three sterile isolators and were orally inoculated with healthy sow fecal suspension on day 7 after birth, which considers as fecal microbiota transplanted (FMT) group. Another six piglets from a natural birth and reared in conventional (CV) environments was regarded as CV group. The FMT piglets were hand-fed Co60-γ-irradiated sterile milk powder, CV piglets were reared by lactating Bama sows and both were weaned at day 21. Then, all piglets were housed separately and fed sterile feed for another 21 days.

Results

We observed that transplanted with sow fecal microbiota increased the content of lipid in liver ($P < 0.05$), and upregulated the mRNA abundances of genes related to lipid anabolism and catabolism in liver and longissimus dorsi of newborn piglets ($P < 0.05$). Meanwhile, the concentrations of adiponectin, GLP-1, and insulin in serum and the activity of CPT-1 in liver were lower in FMT piglets ($P < 0.05$). Besides, transplanted with sow fecal microbiota enhanced the concentration of glycogen in liver ($P < 0.05$), while upregulated the mRNA expressions of genes related to glycogenesis and glycogenolysis in liver and longissimus dorsi of newborn piglets ($P < 0.05$). Moreover, the pathway of AMPK was stimulated by sow fecal microbiota transplantation ($P < 0.10$). In addition, the microbial structure between FMT and CV piglets was marked differently ($P < 0.05$). Furthermore, transplanted with sow fecal microbiota markedly activated the metabolic pathway of bile secretion in newborn piglets ($P < 0.05$).

Conclusions

Collectively, healthy sow gut microbiota transplanted to newborn germ-free piglets might undermine the homeostasis of glucose and lipid metabolism, and increased the content of lipid, and decreased the concentration of glycogen in liver. It is concluded that transplanted with maternal gut microbiota might induce diseases related to glucose and lipid metabolism in newborns.

Introduction

It is important to note that the gut harbors several trillion microbes, which play a crucial role in host health, such as immune, appetite, and energy metabolism [1-4]. Gut microbiota is a vital environmental factor that influences energy harvest from the diet and energy storage to the host [5]. Besides, gut microbiota also contributed to impairing glucose metabolism by stimulating inflammation and macrophage accumulation [6, 7]. Hence, gut microbiota could regulate host lipid and glucose metabolism. Growing circumstantial reports have indicated roles for the gut microbiota in childhood nutrition and growth, as well as in obesity [8, 9]. Noteworthy, decreased bacterial diversity has been

reproducibly observed in people with obesity and type 2 diabetes compared to healthy controls [10, 11]. Increased microbial diversity has been shown to benefit metabolic health [12]. Of note, the gut microbiota of newborns is characterized by low diversity and high instability [13], and the immature gut microbiota could damage the host's growth phenotypes [8]. Importantly, fecal samples from babies and mothers revealed that the diversity of maternal gut microbiota higher than infants [14]. The maternal microbiota is the major microbial source of infant-acquired strains, with maternal gut microbiota providing the largest contribution [15]. Herein, we hypothesized that altered the background microbiota by maternal fecal microbiota transplantation would improve the metabolic health of newborns. An alter gut microbial composition in infants may result in an increased risk of non-communicable diseases, including obesity and metabolic syndrome, allergy-related problems, and diabetes [16, 17]. Therefore, the detailed effects of maternal gut microbiota on the newborns remain obscure, and further research is clearly warranted. Noteworthy, the majority of studies cannot be conducted using human subjects because of ethical considerations. However, animal models can help identify gut microbes and underlying mechanisms. Of note, germ-free (GF) animals are free from living microorganisms, including bacteria, viruses, fungi, protozoa, and parasites throughout their life and reared in sterile environments [18, 19]. The domestic piglet (*Sus scrofa*) is a model of human health, which lies in similar anatomy, physiology, and genetics to humans [20, 21]. Also, the pig eats an omnivorous diet and the developmental phase is similar to that of a human, especially during infancy [22]. Moreover, of the functional pathways observed in the human catalog, 96% were found in the porcine catalog, supporting the potential use of pig for biomedical research [23]. Taken together, we established the CV piglets from a natural birth and sow fecal microbiota transplanted (FMT) piglets which were GF piglets orally infused with healthy sow fecal suspension. The present study was aimed to assess whether maternal gut microbiota has beneficial impacts on newborns in a piglet model. Remarkably, this study might provide novel insights into promoting the metabolic health of newborns.

Results

Serum parameters

According to Table 1, transplanted with sow fecal microbiota decreased the concentrations of adiponectin, GLP-1, and insulin in the serum of newborn piglets ($P < 0.05$).

The contents of lipid and glycogen, and enzyme activity in liver and longissimus dorsi

As presented in Table 2, the content of lipids in liver was higher ($P < 0.05$) and the concentration of glycogen in liver was lower ($P < 0.05$) in FMT group than CV group. Meanwhile, the activity of CPT-1 in liver of FMT group was reduced compared to CV group ($P < 0.05$).

The mRNA expressions of lipid metabolism-related genes in liver and longissimus dorsi

As shown in Table 3, the mRNA abundances of ACC, FAS, and CD36 in liver of FMT group were greater ($P < 0.05$) than CV group. Meanwhile, the mRNA expressions of PNPLA2, CPT-1B, and PGC-1α in liver were

increased ($P < 0.05$) in FMT group. Also, transplanted with sow fecal microbiota enhanced ($P < 0.05$) the mRNA expressions of FAS and LPL, and upregulated ($P < 0.05$) the abundances of PPKAA2 and PNPLA2 in longissimus dorsi of newborn piglets.

The mRNA expressions of glucose metabolism-related genes in liver and longissimus dorsi

According to Table 4, transplanted with sow fecal microbiota upregulated the mRNA expressions of INSR, INS1, PIK3, GYS2, FOXO-1, Sirt1, PCK1, and G6PC in liver of newborn piglets ($P < 0.05$). Moreover, the mRNA abundance of INSR in longissimus dorsi was increased ($P < 0.05$) in FMT group.

The concentrations of adenosine in liver and longissimus dorsi

As presented in Table 5, the concentrations of ADP and AMP, the ratio of AMP to ATP in liver, and the concentrations of ATP, ADP, and AMP in longissimus dorsi were lower in FMT group than CV group ($P < 0.05$). However, the concentration of ATP in liver of FMT group was greater ($P < 0.05$) than CV group.

The protein level associated with lipid and glucose metabolism

As shown in Figure 1, transplanted with sow fecal microbiota stimulated ($P < 0.05$) the protein level of p-AMPK. Likewise, the ratio of p-AMPK to AMPK in FMT group was higher ($P < 0.05$) than CV group. Moreover, the protein level of ACC in FMT group was increased numerically relative to CV group.

16S rRNA analysis of bacterial communities

The relative abundance of gut microbial communities was shown in Figure 2. Ten phyla were chosen for significance analysis. At the phylum level, the colonic samples of conventional CV and FMT piglets were dominated by *Firmicutes*, *Bacteroidetes*, *Proteobacteria*, *Euryarchaeota,* and *Spirochaetes* (Figure 2A). The numerical composition of the bacterial community on the phylum level was analyzed (Table S4), and the abundances of *Firmicutes* and *Bacteroidetes* were markedly decreased ($P < 0.05$) and increased ($P < 0.05$) respectively in FMT group relative to CV group. Besides, FMT piglets had lower ($P < 0.05$) proportions of bacteria in *Spirochaetes* than CV group. At the genera level, the abundances of the top 10 bacterial communities were presented in Figure 2B. The numerical composition of the top 10 bacterial communities on the genera level was analyzed (Table S5). Meanwhile, the proportions of bacteria in *Ruminococcus* and *Treponema* of FMT piglets were lower than ($P < 0.05$) that in CV piglets. Additionally, the proportion of bacteria in *Prevotella* of FMT piglets was increased compared with CV piglets ($P < 0.05$). Notably, the Chao1 and Shannon index of FMT piglets were lower than that in CV piglets ($P < 0.05$) (Figure 3). Moreover, the PCoA and NMDS analyses were carried out to determine the extent of the difference between microbiota communities (Figure 4). The gut microbial communities of CV and FMT piglets could be divided into two different clusters, and the PCoA and NMDS plots showed that bacterial microbiota in the colon of CV and FMT piglets were different clearly.

Metabolomic analysis of the serum samples

To further predict the difference in metabolite profiles related to lipid and glucose metabolism in serum, GC-TOF/MS was used to analyze the metabolite profiles. The PLS-DA (Figure 5) and OPLS-DA (Figure 6) models showed that the two groups were well-separated in serum. To assess which compounds were responsible for the differences between the two groups, the parameters of VIP > 1.0 and adjusted $P < 0.10$ were used as key lineages for separating the serum compounds between the two groups (Figure 7 and Table 6). In total, one hundred and six compounds with a VIP > 1.0 and adjusted $P < 0.10$ were identified. Among these, twenty-six metabolites were enriched ($P < 0.05$), and fifty-seven metabolites were reduced ($P < 0.05$) in FMT group compared with CV group. To comprehensively understand the physiological change induced by oral infusion of sow fecal microbiota, the Kyoto Encyclopedia of Genes and Genomes (KEGG) pathway database was utilized for analyzing related metabolic pathways of 106 metabolites observed in serum. According to Figure 8, these metabolites were involved in multiple biochemical pathways, while the metabolic pathway of central carbon metabolism in cancer was the most significantly affected by oral infusion of sow fecal microbiota, and followed by the metabolic pathway of bile secretion. Eleven metabolites participate in the metabolic pathway of bile secretion. Among them, four metabolites (dopamine, cholic acid, deoxycholic acid, salicylic acid) were enhanced ($P < 0.05$), and four metabolites (choline, alpha-ketoglutarate, lithocholic acid) were reduced ($P < 0.05$) in FMT group relative to CV group.

Discussion

Gut harbors complex communities of microbiota comprising bacteria, fungi, archaea, and yeast, as well as viruses, which perform critical functions in terms of immunity, nutrition, physiology, and metabolism [24]. Destroy gut bacterial communities have been linked to a variety of health conditions [11, 25]. Hence, defining the effects of gut microbiota on the host health is a benefit for understanding the host-microbiota interactions. It is well known that the gut microbiota of newborns is characterized by low diversity and high instability [13]. Conversely, fecal samples from babies and mothers revealed that the diversity of maternal gut microbiota higher than infants [14]. Increased microbial diversity has been shown to benefit metabolic health [12]. Of note, maternal gut microbiota represents the most important microbial source for the development of the neonatal microbiota [15]. Until now, information about the maternal gut microbiota on the metabolic health of neonates is limited, and using a GF piglet model to dissect the detailed effects is scarce. In the present study, we established the CV piglets from a natural birth and FMT piglets which were germ-free piglets orally infused with healthy sow fecal suspension, and aim to test the hypothesis that maternal gut microbiota transplantation may exert beneficial impacts on newborns.

Importantly, acting in peripheral tissues, adiponectin regulated lipid metabolism and influenced energy expenditure [26]. The concentration of adiponectin in serum was reduced in individuals with obesity and obesity-related diseases [27]. Of note, our results showed that transplanted with sow fecal microbiota decreased the concentration of adiponectin in serum, and increased the content of lipid in liver of newborn piglets. Correspondingly, we detected the concentration of ATP in liver of FMT group was greater than CV group. Thus, these suggested that transplanted with maternal fecal microbiota might aggravate

the fat deposition of newborns. Indeed, we observed the final body weight of FMT piglets were greater than CV piglets (data unpublished). Moreover, the activity of CPT-1 in liver was decreased and the mRNA expressions of FAS, ACC, and CD36 in liver were markedly upregulated in the FMT group. Notably, CPT-1 is the rate-limiting enzyme that determines fatty acid oxidation [28]. FAS is the pivotal enzyme that catalyzes fatty acid synthesis [29]. ACC modulates fatty acids metabolism, and its product (e.g. malonyl-CoA) serves as a building block for de novo fatty acid synthesis [30]. Meanwhile, CD36, the fatty acid translocase, regulates the uptake of long-chain fatty acids into cells [31] and elevates expression of CD36 in various tissues result in lipid overload and lipotoxicity [32]. Similarly, in our study, the mRNA abundances of FAS and LPL in longissimus dorsi of FMT group were higher than CV group. The function of LPL catalyzes the hydrolysis of triglycerides residing in chylomicrons and providing free fatty acid for tissue utilization [28]. Intriguingly, we also measured the mRNA expressions of CPT-1B, PNPLA2, and PGC-1α in liver, PPKAA2 and PNPLA2 in longissimus dorsi were increased in FMT group. The PNPLA2 gene encodes adipose triglyceride lipase, which is the rate-limiting enzyme for the hydrolysis of intracellular triglyceride [33]. The PGC-1α is measured as a vital regulator of fatty acid metabolism [34], and demonstrated the protective role against hepatic steatosis [35]. Additionally, PGC-1α expression in liver was a negative association with body fat [36, 37]. The PPKAA2 is one subunit of adenosine monophosphate-activated protein kinase (AMPK), which is mainly distributed in liver and skeletal muscle [38]. Increased activation of AMPK could promote fatty acid oxidation and reduce lipid deposition [39]. In the present study, we observed the protein level of p-AMPK in liver tended to increase in FMT group, and the ratio of p-AMPK/AMPK was markedly higher than CV group. Collectively, transplanted with sow fecal microbiota might regulate the lipid anabolism and catabolism of newborns, and enhanced the lipid accumulation in liver ultimately.

The liver acts as a central role in regulating blood glucose homeostasis by uptake of glucose in the postprandial state and conversion to glycogen and triglyceride, and by the production of glucose in the postabsorptive state through glycogenolysis and gluconeogenesis [40, 41]. It is well established that insulin resistance and hepatic steatosis lead to compromised glycogen synthesis [42, 43]. Whereas increased liver glycogen synthesis could improve glucose tolerance [44]. Moreover, our results showed that transplanted with sow fecal microbiota decreased the concentrations of GLP-1 and insulin in serum. As is known to us, GLP-1 could inhibit glucagon secretion and improve insulin sensitivity [45]. In addition, the mRNA expression of GSK3 in liver was tended to upregulated in FMT group. GSK3 could inhibit glycogen synthase activity by phosphorylating it, thereby reducing glycogen synthesis [46]. These demonstrated that transplanted with sow gut microbiota might impair glucose control and decrease the insulin sensitivity of newborn piglets. Verifiably, our results observed the mRNA abundances of INSR, INS1, and PIK3 in liver were increased in FMT group. Analogously, in the longissimus dorsi, the mRNA abundance of INSR was stimulated and PI3K was tended to upregulate in FMT group. The insulin receptor substrates bind to the activated insulin receptor, then are phosphorylated, thereby providing docking sites for a multitude of signaling molecules (e.g. PIK3), essential for the diversification and regulation of insulin action, and hence for the tight modulation of the hepatic glucose [47].On the contrary, transplanted with sow fecal microbiota also increased the mRNA abundances of GYS2, PCK1,

and G6PC. The rate-limiting enzyme for glycogen synthesis is glycogen synthase (GS), in mammals, there are two GS isoforms: muscle GS (encoded by GYS1), which is abundantly expressed in skeletal and cardiac muscles, and the liver-restricted isoform (encoded by GYS2) [48]. Previous work indicated that mice lacked GYS2 had a severe decrease in their ability to store glycogen in hepatocytes [48]. The two rate-limiting enzymes known to act important roles in gluconeogenesis are phosphoenolpyruvate carboxykinase (PCK) and glucose-6-phosphatase (G6Pase) [49, 50]. The G6PC catalyzes the hydrolysis of glucose-6-phosphate to glucose and phosphate in the final step of gluconeogenesis [51]. In addition, upregulated the mRNA expression of hepatic PCK1 reduced plasma glucose in mice [52]. However, in the current study, the content of glycogen in liver was reduced in FMT group. Therefore, these indicated that maternal gut microbiota could regulate glucose metabolism and decreased liver glycogen of newborns in the piglet model.

In the present study, the GF newborn piglets were transplanted with the healthy Bama sow donor fecal microbiota, while the microbiota diversity indices of Shannon and Chao1 in FMT piglets were significantly lower than CV piglets. The possible influence of the microbiota community on energy harvest has been considered as the potential contribution to obesity [53]. A previous study indicated that obese mice contained more *Firmicutes* and fewer *Bacteroidetes* in cecum than lean wild-type controls [54]. Similar results also have been found in the fecal microbiota of humans who are obese [55]. However, other human research demonstrated the opposite result [56], or no difference [57]. Indeed, our results indicated that the fat deposition in liver of FMT piglets was markedly increased, while the abundance of *Bacteroidetes* was upregulated compared to CV piglets. Moreover, in the present study, the abundances of *Bacteroides* and *Prevotella* in FMT were greater than CV piglets, while increased levels of *Bacteroides* and *Prevotella* were reported negatively correlated with energy intake and adiposity [58]. Additionally, improved tolerance to glucose could be explained largely through the enrichment of the genus *Prevotella* within the microbiota [59]. However, the content of glycogen in liver and insulin concentration in serum of FMT piglets were lower than CV piglets. On the other hand, the *Ruminococcaceae* and *Spirochaetes* were considered to degrade macromolecular polymers and improve the digestibility of the complex components of dietary fiber [11, 60]. Unfortunately, the abundances of *Ruminococcaceae* and *Spirochaetes* in FMT group were lower than CV group. Herein, these suggested that transplanted with maternal gut microbiota might increase the risk of obesity in newborns by changing the microbial community.

According to the preceding results of the present study, we have obtained that transplanted with maternal gut microbiota significantly affected the lipid and glucose metabolism in the piglet model. However, the knowledge of the exact mode of action remains largely unknown. In the current study, metabolomic based on UHPLC-Q-TOF/MS was performed to elucidate the underlying mechanism of transplanted with maternal gut microbiota on lipid and glucose metabolism. It is well known that serum can be regarded as a metabolic fingerprint that provides a visual result of the metabolic events and reveals changes in metabolic pathways under various nutritional or physiological conditions [61]. In the present study, PLS-DA and OPLS-DA analyses demonstrated a clear separation of serum metabolites due to infused with maternal fecal microbiota, suggesting marked differences in the metabolic profiles. Besides, taken KEGG

pathway analysis, we observed the metabolic pathway of bile secretion in piglets was apparently affected by transplanted with sow fecal microbiota. Bile acids, produced by the microbiota from host cholesterol, are the important metabolites with a profound impact on human health [62]. Moreover, they serve as signaling molecules and bind to cellular receptors such as the bile-acid-synthesis controlling nuclear receptor farnesoid X receptor (FXR) and G-protein-coupled bile acid receptor 1 (also known as TGR5) [63]. Noteworthy, both FXR and TGR5 have been indicated in the regulation of glucose metabolism in mice, but FXR impairs, whereas TGR5 improves, glucose homeostasis [64, 65]. Compared to FXR, which is activated by primary bile acids, TGR5 binds secondary bile acids such as deoxycholic acid (produced from cholic acid) and lithocholic acid (produced from chenodeoxycholic acid). Intriguingly, in the present study, the contents of deoxycholic acid and cholic acid were significantly increased, while the concentration of lithocholic acid was markedly decreased in FMT group. Notably, TGR5 signaling in enteroendocrine L-cells promotes secretion of GLP-1, thereby enhancing liver and pancreatic function and increasing glucose tolerance in obese mice [65]. In addition, activation of TGR5 in muscle and brown adipose tissue induces energy expenditure and prevents diet-induced obesity [66]. On the other hand, the concentration of choline in FMT group was apparently lower than CV group. Remarkably, choline was significant for lipid metabolism in the liver, reduced the levels of bioavailable choline were suggested to trigger non-alcoholic fatty liver disease in mice [67]. Consequently, these might indicate that the underlying mechanism of transplanted with sow fecal microbiota regulated piglet's lipid and glucose metabolism was through the metabolic pathway of bile secretion.

Conclusions

In summary, the present study indicated that transplanted with sow gut microbiota might aggravate the fat deposition and undermine glucose control in newborn piglets. It is concluded that recolonize with maternal gut microbiota might impair the metabolic health of newborns. This work also facilitated the research of the interactions between microbiota and host and contributed to the studies of human maternal gut microbiota transplanted to the germ-free piglet model.

Material And Methods

Preparation of fecal microbiota suspension

According to the standard for donor identification and screening described previously [68], healthy multiparous Bama sows (n = 6) without antibiotics and probiotics treated within three months were used as fecal donors. The analysis of *Actinobacillus pleuropneumoniae*, *Brucellosis*, *Helminths*, *Eimeria*, *Coccidia*, *Serpulinhyodysen*, porcine parvovirus, porcine epidemic diarrhea virus, and transmissible gastroenteritis virus in feces of donor sows were negative (Xishan Biotechnology Inc. Suzhou China). The fresh feces of sows were collected after 12 h fasting, and the sow fecal suspension was prepared following Zeng et al. (2013) [69].

Experimental animals, design, and diets

Six GF piglets were delivered by hysterectomy from a multiparous Bama sow (a native breed of China). At 112 days of gestation (full-term, 114 days), pregnant Bama sows were anesthetized with 4% isoflurane, the uterus was excised from the anesthetized sow and was transferred into a sterile isolator (DOSSY Experimental Animals Co., Ltd, Chengdu, China) through a tank including 120 L of 0.1% peracetic acid for decontamination of the uterus. Then the piglets were taken from the uterus in the isolator and the six neonatal piglets (gilts and boars in half) were transferred to three rearing isolators (Class Biologically Clean Ltd., Madison, Wisconsin, USA). The isolator has a checkboard and piglets were fed separately. The rearing isolators had been sterilized by spraying with 1% peracetic acid in advance and maintained in sterile environments as described previously [19]. On the 7th day after birth, six GF piglets were orally infused with healthy donor sow fecal suspension, and with 1 ml/piglet/day for three days. These piglets were designated as FMT group and were hand-fed Co60-γ-irradiated sterile milk powder (Table S1) diluted with sterile water (1:4) for 21 days. Another six piglets (gilts and boars in half) were generated by natural birth from a multiparous Bama sow were regarded as CV group and reared by lactating Bama sows for 21 days, then transferred to and fed in single cage respectively. A corn-soybean feed formulated according to NRC (2012) requirements and Chinese feeding standards for local piglets (2004) (Table S2) was sterilized by Co60-γ-radiation and introduced to the CV and FMT piglets for another 21 days. In the two 21-days periods, all piglets were allowed *ad libitum* access to water.

Sample collection

Before the piglets were euthanized, blood samples were obtained from anterior vena cava before euthanized via isoflurane anesthesia on the 42th day of the experiment, centrifuged at 3,000 g for 15 min, and stored at -80 °C for further analysis. The abdomen was opened immediately, and the digesta samples in the proximal colon of CV and FMT piglets were collected and frozen at -80 °C until for bacterial community measurement. This was followed by collecting the tissues of the liver and longissimus dorsi and stored at -80 °C for further measurements.

Serum biochemical analyses

The concentrations of adiponectin, insulin, glucagon, glucagon-like peptide 1, and leptin in serum were detected by commercial enzyme-linked immunosorbent assay (ELISA) kits from Chenglin Co. Ltd. (Beijing, China) according to the manufacturer's instructions. The concentrations of total cholesterol (TC), triglyceride (TG), high density lipoprotein-cholesterol (HDL-c), low density lipoprotein-cholesterol (LDL-c), and glucose in serum were measured using commercial kits (Nanjing Jiancheng Bioengineering Institute, Nanjing, China) following with the manufacturer’s instructions. Each parameter was measured in triplicate simultaneously on the same plate. And the differences among parallels must be small (coefficient of variation was less than 10%) to guarantee the reproducibility of repeated measurements.

Measurement of lipid and glycogen contents

The contents of lipid in liver and longissimus dorsi were measured by a Soxhlet extraction procedure using petroleum ether as an extraction agent. The concentrations of glycogen in liver and longissimus

dorsi were analyzed using the commercial kit (Nanjing Jiancheng Bioengineering Institute, Nanjing, China) according to the manufacturer's instructions.

Determination of enzyme activity

About 1000 mg frozen sample of liver and longissimus dorsi were homogenized in ice-cold saline solution (1:9, wt/vol) and then centrifuged at 3,000×g for 15 min at 4℃. The supernatant was collected for further analysis. The activities of carnitine palmitoyltransferase 1 (CPT-1), lipoprotein lipase (LPL), hepatic lipase (HL), and malate dehydrogenase (MDH) in liver and longissimus dorsi were determined using commercial kits (Nanjing Jiancheng Bioengineering Institute, Nanjing, China) following with the manufacturer's instructions. The total protein content in liver and longissimus dorsi homogenates was detected by Bradford brilliant blue method [70]. Each parameter was determined in triplicate simultaneously on the same plate. And the differences among parallels must be small (coefficient of variation was less than 10%) to guarantee the reproducibility of repeated measurements.

Real-time quantitative PCR

Total RNA was isolated from frozen liver and longissimus dorsi, using Trizol reagent (TaKaRa) according to the manufacturer's instructions. The concentration and purity of the RNA were determined using a NanoDrop ND-2000 Spectrophotometer (NanoDrop, Germany). Ratios of OD_{260}:OD_{280} ranging from 1.8 to 2.0 in all samples were regarded as suitable for further analysis. The integrity of RNA was detected by agarose gel electrophoresis and the 28S:18S ribosomal RNA band ratio was determined as ≥1.8. RNA was reverse transcribed into cDNA using the PrimeScriptTM RT reagent kit (TaKaRa) according to the manufacturer's guidelines. Primers for the selected genes (Supplementary Table S3) were designed by Primer 6 Software (PREMIER Biosoft International, Palo Alto, CA, USA) and synthesized commercially by Sangon Biotech Limited (Shanghai, China). The Quantitative real-time PCR was performed on an ABI Prism 7000 detection system in a two-step protocol with SYBR Green (Applied Biosystems, Foster City, CA, USA). Each reaction was performed in a volume of with 1 μl of cDNA, 5 μl of SYBR Premix Ex Taq TM (2×), 0.2 μl of ROX reference dye (50×), 0.4 μl of each forward and reverse primer, and 3 μl of PCR-grade water. The PCR conditions were as follows: initial denaturation at 95 °C for 30 s, followed by 40 cycles of denaturation at 95 °C for 10 s, annealing at 60 °C for 25 s, and a 72 °C extension step for 5 min. A melting curve analysis was generated following each Quantitative real-time PCR assay to verify the specificity of the reactions. The housekeeping gene β-actin was chosen as the reference gene to normalize mRNA expression of target genes. Gene expression data of replicate samples was calculated using the $2^{-\Delta\Delta CT}$ method [71]. The relative expression of target genes in the CV group was set to be 1.0. Each sample was measured in triplicate.

Analysis of adenosine

The sample of liver or longissimus dorsi (100 mg) was homogenized with 5 mL of 0.4 M perchloric acid at 0 ℃ for 1 min, and with ultrasonic treatment for 30 min. Then, the mixture was centrifuged at 3,000 g for 10 min. and the supernatant immediately neutralized to pH 6.5 with 50 mM monopotassium

phosphate. After that, monopotassium phosphate was removed by filtration through the sintered glass and stored at -80 ℃ for subsequent analysis. The high-performance liquid chromatography (HPLC, U3000, Thermo Fisher Scientific, USA) was used to determine the concentrations of adenosine triphosphate (ATP), adenosine diphosphate (ADP), and adenosine monophosphate (AMP) in liver and longissimus dorsi [72].

Determination of protein levels by western blot

The antibodies against β-actin, GPR43, p-AMPK, AMPK, GSK3-α, CPT-1B, and ACC were obtained from Cell Signaling Technology (Davers, MA), Abcam (Cambridge, MA, USA), and Santa Cruz Biotechnology Inc. (Santa Cruz, CA, USA), respectively. Protein levels for the β-actin, GPR43, p-AMPK, AMPK, GSK3-α, CPT-1B, and ACC in the liver were measured by western blot analysis according to the instructions described by Suryawan et al. (2001) [73].

Determination of bacterial community and data analysis

The total DNA of each digesta sample was isolated using the QIAamp stool DNA Mini kit (QIAGEN, Valencia, CA, USA). The concentration and purity of genomic DNA were detected by NanoDrop ND-2000 Spectrophotometer (NanoDrop, Hilden, Germany). The integrity of genomic DNA was measured using electrophoresis on 1% agarose gels. Sequencing was determined by the Novogene Bioinformatics Technology Co. Ltd. (Beijing, China). DNA library was generated before high-throughput sequencing as previously reported [74]. The library was sequenced on the Illumina HiSeq platform and using a 250-bp paired-end reads strategy. The resulting sequences were clustered into operational taxonomic units (OTUs) using USEARCH drive at 97% sequence similarity, and a representative sequence was selected. The relative abundance of each OTU was examined at different taxonomic levels. Species annotation of OTU representative sequences was identified with the RDP Classifier method and Green Gene database. The populations of the bacterial community in colonic digesta of weaned piglets at the phyla, class, order, family, and genera levels, and the Alpha diversity index of Chao1 and Shannon were measured by the method of Kruskal–Wallis. The abundances of bacteria at the phylum, class, order, and family levels were shown as bar plots. The Beta diversity included principal co-ordinates analysis (PCoA) and non-metric multidimensional scaling (NMDS), and the plots were produced by Euclidean distances and Bray-Curtis distances respectively. The plots were visualized using R software (Package ape).

Ultrahigh-performance liquid chromatography equipped with quadrupole time of-flight mass spectrometry (UHPLC-Q-TOF/MS) analysis and data analysis

The UHPLC-Q-TOF/MS analysis was performed with an Agilent 1290 UHPLC system (Agilent, Palo Alto, USA) and combined with a Q-TOF mass spectrometer (ESI/Triple TOF 5600; AB Sciex, Concord, Canada) were used to measure the serum metabolites. For the serum samples, the pretreatment, extraction, and identification were according to the procedure described by Hu et al. (2019) [75]. The raw data (whiff scan files) were converted into mzXML format using ProteoWizard [76] and were imported to the XCMS software for peak matching, retention time alignment, and peak area extraction [77]. Metabolite structure

identification was performed by comparing the accuracy of m/z values (< 25 ppm), and MS/MS spectra were interpreted with an in-house database (Shanghai Applied Protein Technology Co. Ltd, China) established with authentic standards. For the XCM data, the ion peaks that were missing values greater than 50% in the group were filtered and excluded and data were normalized to total peak intensity. Then, statistical analyses were performed using SIMCA-P software (version 14.1, Umetrics, Umea, Sweden), where could subjected to multivariate data analysis, including partial least squares discriminant analysis (PLS-DA) and orthogonal partial least squares discriminant analysis (OPLS-DA), which were carried out to uncover and extract the statistically significant metabolite variations. The PLS-DA and OPLS-DA models were validated based on multiple correlation coefficient (R^2) and cross-validated (Q^2) in cross-validation and permutation test by applying 2000 iterations [78]. The R^2 value in the permutated plot described how well the data fit the derived model, whereas the Q^2 value described the predictive ability of the constructed model and was a measure of model quality [79]. The significance of the biomarkers was ranked using the variable importance in the projection (VIP) score (>1) from the OPLS-DA model. Metabolites with the highest VIP score are the most powerful group discriminators, VIP score > 1 are significant [80]. The procedure of metabolites identification and pathway analysis was according to Wang et al. (2017) [78]. Metabolites with a VIP score >1 was further analyzed by the Student's *t*-test at the univariate level to measure the significance of each metabolite. The univariate data analysis also included a fold-change analysis.

Statistical analysis

All data were analyzed in SAS 9.2 (SAS Institute, Inc., Cary, NC, USA) and analyzed using Student's *t*-test, and were presented as means ± SEMs. $P < 0.05$ was considered to be statistically significant, and tendency was declared with $0.05 < P < 0.10$.

Declarations

Acknowledgements

Not applicable.

Funding

This study was supported by National Natural Science Foundation of China (31730091) and the National Key Research and Development Program of China (2017YFD0500503).

Availability of data and materials

The data were exhibited in the main manuscript and supplemental materials.

Author Contributions

H.Z. conducted the animal work and the laboratory work, and wrote the manuscript. H.Z., L.G. and D.C. designed the experiment. B.Y. and J.S. gave advice on the experiment design. H.Z. analyzed the study data and wrote the manuscript. Z.L. and H.C. helped to revise the manuscript. All the authors have read and approved the final manuscript.

Ethics approval

Experimental protocols and procedures used in the present experiment were approved by the Animal Care and Use Committee of Sichuan Agricultural University (Chengdu, China) under permit number DKY-B20131704. The experiment was carried out at the Experimental Swine Engineering Center of the Chongqing Academy of Animal Sciences (CMA No. 162221340234; Chongqing, China).

Consent for publication

Not applicable.

Competing interests

All authors declare that they have no competing interest in the present work.

References

[1] Kamada N, Chen GY, Inohara N, Núñez G. Control of pathogens and pathobionts by the gut microbiota. Nat Immunol. 2013;14(7):685-90.

[2] Yano J, Yu K, Donaldson G, Shastri G, Ann P, Ma L, et al. Indigenous bacteria from the gut microbiota regulate host serotonin biosynthesis. Cell. 2015;161(2):264-76.

[3] Haiser HJ, Gootenberg DB, Chatman K, Sirasani G, Balskus EP, Turnbaugh PJ. Predicting and manipulating cardiac drug inactivation by the human gut bacterium Eggerthella lenta. Science. 2013;341(6143):295-8.

[4] Yatsunenko T, Rey FE, Manary MJ, Trehan I, Dominguezbello MG, Contreras M, et al. Human gut microbiome viewed across age and geography. Nature. 2012;486(7402):222-7.

[5] Bäckhed F, Ding H, Wang T, Hooper LV, Koh GY, Nagy A, et al. The gut microbiota as an environmental factor that regulates fat storage. Proc. Natl. Acad. Sci. U. S. A. 2004;101(44):15718-23.

[6] Caesar R, Reigstad C, Bäckhed H, Reinhardt C, Ketonen M, Lundén G, et al. Gut-derived lipopolysaccharide augments adipose macrophage accumulation but is not essential for impaired glucose or insulin tolerance in mice. Gut. 2012;61:1701-7.

[7] Cani PD, Amar J, Iglesias MA, Poggi M, Knauf C, Bastelica D, et al. Metabolic endotoxemia initiates obesity and insulin resistance. Diabetes. 2007;56(7):1761-72.

[8] Blanton LV, Charbonneau MR, Salih T, Barratt MJ, Venkatesh S, Ilkaveya O, et al. Gut bacteria that prevent growth impairments transmitted by microbiota from malnourished children. Science. 2016;351(6275). doi: 10.1126/science.aad3311.

[9] Charbonneau MR, O'Donnell D, Blanton LV, Totten SM, Davis JC, Barratt MJ, et al. Sialylated Milk oligosaccharides promote microbiota-dependent growth in models of infant undernutrition. Cell. 2016(5);164:859-71.

[10] Lambeth SM, Carson T, Lowe J, Ramaraj T, Leff JW, Luo L, et al. Composition, diversity and abundance of gut microbiome in prediabetes and type 2 diabetes. J Diabetes Obesity. 2015;2(3):1-7.

[11] Turnbaugh PJ, Hamady M, Yatsunenko T, Cantarel BL, Duncan A, Ley RE, et al. A core gut microbiome in obese and lean twins. Nature. 2009;457(7228):480-4.

[12] Chatelier EL, Nielsen T, Qin J Prifti E, Hildebrand F, Falony G, et al. Richness of human gut microbiome correlates with metabolic markers. Nature 2013;500(7464):541-6

[13] Parker A, Lawson M, Vaux L, Pin C. Host-microbe interaction in the gastrointestinal tract. Environ Microbiol. 2018;20(7):2337-53.

[14] Yan SCF, Tsaliki E, Vervier K, Strang A, Simpson N, Kumar N, Stares MD, Rodger A, Brocklehurst P, Field N, Lawley TD. Stunted microbiota and opportunistic pathogen colonisation in caesarean section birth. Nature. 2019;574(7776):117-21.

[15] Ferretti P, Pasolli E, Tett A, Asnicar F, Gorfer V, Fedi S, et al. Mother-to-infant microbial transmission from different body sites shapes the developing infant gut microbiome. Cell Host Microbe. 2018;24(1):133-45.

[16] Kwon EJ, Kim YJ. What is fetal programming?: a lifetime health is under the control of in utero health. Obstet Gynecol Sci. 2017;60(6):506-19.

[17] Dominguez-Bello MG, Costello EK, Contreras M, Magris M, Hidalgo G, Fierer N, et al. Delivery mode shapes the acquisition and structure of the initial microbiota across multiple body habitats in newborns. Proc Natl Acad Sci U S A. 2010;107(26):11971-5.

[18] Delzenne NM, and Cani, P. D. Interaction between obesity and the gut microbiota: relevance in nutrition. Annu Rev Nutr. 2011;31(15-31):1-7.

[19] Meyer R, Bohl E, Kohler E. Procurement and Maintenance of Germ-Free Swine for Microbiological Investigations. Appl Microbiol. 1964;12:295-300.

[20] Meurens FO, Summerfield A, Nauwynck H, Saif L, Gerdts V. The pig: a model for human infectious diseases. Trends Microbiol. 2012;20(1):50-7.

[21] Odle J, Lin X, Jacobi SK, Kim SW, Stahl CH. The suckling piglet as an agrimedical model for the study of pediatric nutrition and metabolism. Annu Rev Anim Biosci. 2014;2(1):419-44.

[22] Garthoff LH, Henderson GR, Sager AO, Sobotka TJ, Khan MA. The Autosow raised miniature swine as a model for assessing the effects of dietary soy trypsin inhibitor. Food Chem Toxico. 2002;40(4):487-500.

[23] Liang X, Estellé J, Kiilerich P, Ramayo-Caldas Y, Xia Z, Feng Q, et al. A reference gene catalogue of the pig gut microbiome. Nat Microbiol. 2016;1:16161.

[24] Milani C, Duranti S, Bottacini F, Casey E, Turroni F, Mahony J, et al. The First Microbial Colonizers of the Human Gut: Composition, Activities, and Health Implications of the Infant Gut Microbiota. Microbiol Mol Biol Rev. 2017;81(4):e00036-17.

[25] Hakansson A, Molin G. Gut Microbiota and Inflammation. Nutrients. 2011;3(6):637-82.

[26] Liu M, Liu F. Regulation of adiponectin multimerization, signaling and function. Best Pract Res Clin Endocrinol Metab. 2014;28:25-31.

[27] Arita Y, Kihara S, Ouchi N, Takahashi M, Maeda K, Miyagawa J, et al. Paradoxical decrease of an adipose-specific protein, adiponectin, in obesity. Biochem Biophys Res Commun. 1999;257(1):79-83.

[28] Snel M, Jonker JT, Schoones J, Lamb H, Jazet IM. Ectopic fat and insulin resistance: pathophysiology and effect of diet and lifestyle interventions. Int J Endocrinol. 2012;2012(7):983814.

[29] Yan H, Zheng P, Yu B, Yu J, Mao X, He J, et al. Postnatal high-fat diet enhances ectopic fat deposition in pigs with intrauterine growth retardation. Eur J Nutr. 2017;56(2):483-90.

[30] Kim KH. Regulation of mammalian acetyl-coenzyme A carboxylase. Annu Rev Nutr. 2003;17(1):77-99.

[31] Febbraio M, Hajjar DP, Silverstein RL. CD36: a class B scavenger receptor involved in angiogenesis, atherosclerosis, inflammation, and lipid metabolism. J Clin Invest. 2001;108(6):785-91.

[32] Bonen A, Parolin ML, Steinberg GR, Calles-Escandon J, Tandon NN, Glatz JF, et al. Triacylglycerol accumulation in human obesity and type 2 diabetes is associated with increased rates of skeletal muscle fatty acid transport and increased sarcolemmal FAT/CD36. FASEB J. 2004;18(10):1144-6.

[33] Fischer J, Lefèvre C, Morava E, Mussini JM, Laforêt P, Negre-Salvayre A, et al. The gene encoding adipose triglyceride lipase (PNPLA2) is mutated in neutral lipid storage disease with myopathy. Nature Gene. 2007;39(1):28-30.

[34] Vega RB, Huss JM, Kelly DP. The coactivator PGC-1 cooperates with peroxisome proliferator-activated receptor alpha in transcriptional control of nuclear genes encoding mitochondrial fatty acid oxidation enzymes. Mol Cell Biol. 2000;20(5):1868-76.

[35] Estall JL, Kahn M, Cooper MP, Fisher FM, Wu MK, Laznik D, et al. Sensitivity of lipid metabolism and insulin signaling to genetic alterations in hepatic peroxisome proliferator-activated receptor-gamma coactivator-1alpha expression. Diabetes. 2009;58(7):1499-508.

[36] Balampanis K, Chasapi A, Kourea E, Tanoglidi A, Hatziagelaki E, Lambadiari V, et al. Inter-tissue expression patterns of the key metabolic biomarker PGC-1α in severely obese individuals: Implication in obesity-induced disease. Hellenic J Cardiol. 2019;60(5):282-93.

[37] Besse-Patin A, Léveillé M, Oropeza D, Nguyen BN, Prat A, Estall JL. Estrogen signals through peroxisome proliferator-activated receptor-γ coactivator 1α to reduce oxidative damage associated with diet-induced fatty liver disease. Gastroenterology. 2017;152(1):243-56.

[38] Dyck JR, Kudo N, Barr AJ, Davies SP, Hardie DG, Lopaschuk GD. Phosphorylation control of cardiac acetyl-CoA carboxylase by cAMP-dependent protein kinase and 5'-AMP activated protein kinase. Eur J Biochem. 1999;262(1):184-90.

[39] Samuel BS, Shaito A, Motoike T, Rey FE, Backhed F, Manchester JK, et al. Effects of the gut microbiota on host adiposity are modulated by the short-chain fatty-acid binding G protein-coupled receptor, Gpr41. Proc Natl Acad Sci U S A. 2008;105(43):16767-72.

[40] Wasserman DH. Four grams of glucose. Am J Physiol Endocrinol Metab. 2009;296(1):E11-21.

[41] Agius L. Physiological control of liver glycogen metabolism: lessons from novel glycogen phosphorylase inhibitors. Mini Rev Med Chem. 2010;10(12):1175-87.

[42] Samuel VT, Liu ZX, Qu X, Elder BD, Bilz S, Befroy D, et al. Mechanism of hepatic insulin resistance in non-alcoholic fatty liver disease. J Biological Chem. 2004;279(31):32345-53.

[43] Petersen KF, Dufour S, Savage DB, Bilz S, Solomon G, Yonemitsu S, et al. The role of skeletal muscle insulin resistance in the pathogenesis of the metabolic syndrome. Proc Natl Acad Sci U S A. 2007;104(31):12587-94.

[44] Ros S, Zafra D, Valles-Ortega J, García-Rocha M, Forrow S, Domínguez J, et al. Hepatic overexpression of a constitutively active form of liver glycogen synthase improves glucose homeostasis. J Biological Chem. 2010;285(48):37170-7.

[45] Diamant M, Bunck MC, Heine RJ. Analogs of glucagon-like peptide-1 (GLP-1): an old concept as a new treatment of patients with diabetes mellitus type 2. Ned Tijdschr Geneeskd. 2004;148(39):1912-7.

[46] Lee J, Kim MS. The role of GSK3 in glucose homeostasis and the development of insulin resistance. Diabetes Res Clin Pract. 2007;77(Suppl 1):S49-57.

[47] Fritsche L, Weigert C, Haring H-U, Lehmann R. How insulin receptor substrate proteins regulate the metabolic capacity of the liver - implications for health and disease. Curr Med Chem. 2008;15(13):1316-

29.

[48] Irimia JM, Meyer CM, Peper CL, Zhai L, Bock CB, Previs SF, et al. Impaired glucose tolerance and predisposition to the fasted state in liver glycogen synthase knock-out mice. J Biological Chem. 2010;285(17):12851-61.

[49] Choi MS, Jung UJ, Yeo J, Kim MJ, Lee MK. Genistein and daidzein prevent diabetes onset by elevating insulin level and altering hepatic gluconeogenic and lipogenic enzyme activities in non-obese diabetic (NOD) mice. Diabete Res Rev. 2008;24(1):74-81.

[50] Seo KI, Choi MS, Jung UJ, Kim HJ, Yeo J, Jeon SM, et al. Effect of curcumin supplementation on blood glucose, plasma insulin, and glucose homeostasis related enzyme activities in diabetic db/db mice. Mol Nutr Food Res. 2008;52(9):995-1004.

[51] Chou JY, Mansfield BC. Mutations in the glucose-6-phosphatase-alpha (G6PC) gene that cause type Ia glycogen storage disease. Hum Mutat. 2010;29(7):921-30.

[52] Yuan X, Dong D, Li Z, Wu B. Rev-erbα activation down-regulates hepatic Pck1 enzyme to lower plasma glucose in mice. Pharmacol Res. 2019;141:310-8.

[53] Ze X, Duncan SH, Louis P, Flint HJ. Ruminococcus bromii is a keystone species for the degradation of resistant starch in the human colon. ISME J. 2012;6(8):1535-43.

[54] Ley RE, Bäckhed F, Turnbaugh P, Lozupone CA, Knight RD, Gordon JI. Obesity alters gut microbial ecology. Proc Natl Acad Sci U S A. 2005;102(31):11070-5.

[55] Ley RE, Turnbaugh PJ, Klein S, Gordon JI. Microbial ecology: human gut microbes associated with obesity. Nature. 2006;444(7122):1022-3.

[56] Schwiertz A, Taras D, Schäfer K, Beijer S, Bos NA, Donus C, et al. Microbiota and SCFA in lean and overweight healthy subjects. Obesity. 2010;18(1):190-5.

[57] Duncan SH, Lobley GE, Holtrop G, Ince J, Johnstone AM, Louis P, et al. Human colonic microbiota associated with diet, obesity and weight loss. Int J Obes (Lond). 2008;32(11):1720-4.

[58] Furet JP, Kong LC, Tap J, Poitou C, Basdevant A, Bouillot JL, et al. Differential adaptation of human gut microbiota to bariatric surgery-induced weight loss: links with metabolic and low-grade inflammation markers. Diabetes. 2010;59(12):3049-57.

[59] Kovatcheva-Datchary P, Nilsson A, Akrami R, Lee YS, De Vadder F, Arora T, et al. Dietary fiber-induced improvement in glucose metabolism is associated with increased abundance of prevotella. Cell Metab. 2015;22(6):971-82.

[60] Lilburn TG, Schmidt TM, Breznak JA. Phylogenetic diversity of termite gut spirochaetes. Environ Microbiol. 1999;1(4):331-45.

[61] Ramsay TG, Stoll MJ, Shannon AE, Blomberg LA. Metabolomic analysis of longissimus from underperforming piglets relative to piglets with normal preweaning growth. J Anim Sci Biotechnol. 2018;9:36.

[62] Russell DW. The enzymes, regulation, and genetics of bile acid synthesis. Annu Rev Biochem. 2003;72:137-74.

[63] Thomas C, Pellicciari R, Pruzanski M, Auwerx J, Schoonjans K. Targeting bile-acid signalling for metabolic diseases. Nat Rev Drug Discovery. 2008;7(8):678-93.

[64] Prawitt J, Abdelkarim M, Stroeve JH, Popescu I, Duez H, Velagapudi VR, et al. Farnesoid X receptor deficiency improves glucose homeostasis in mouse models of obesity. Diabetes. 2011;60(7):1861-71.

[65] Thomas C, Gioiello A, Noriega L, Strehle A, Oury J, Rizzo G, et al. TGR5-mediated bile acid sensing controls glucose homeostasis. Cell Metab. 2009;10(3):167-77.

[66] Watanabe M, Houten SM, Mataki C, Christoffolete MA, Kim BW, Sato H, et al. Bile acids induce energy expenditure by promoting intracellular thyroid hormone activation. Nature. 2006;439(7075):484-9.

[67] Dumas ME, Barton RH, Toye A, Cloarec O, Blancher C, Rothwell A, et al. Metabolic profiling reveals a contribution of gut microbiota to fatty liver phenotype in insulin-resistant mice. Proc. Natl Acad Sci U S A. 2006;103(33):12511-6.

[68] Hamilton MJ, Weingarden AR, Sadowsky MJ, Khoruts A. Standardized frozen preparation for transplantation of fecal microbiota for recurrent clostridium difficile Infection. Am J Gastroenterology. 2012;107(5):761.

[69] Zeng B, Li G, Yuan J, Li W, Tang H, Wei H. Effects of age and strain on the microbiota colonization in an infant human flora-associated mouse model. Curr Microbiol. 2013;67(3):313-21.

[70] Chen J, Li Y, Yu B, Chen D, Mao X, Zheng P, et al. Dietary chlorogenic acid improves growth performance of weaned pigs through maintaining antioxidant capacity and intestinal digestion and absorption function. J Anim Sci. 2018;96(3):1108-18.

[71] Pfaffl MW. A new mathematical model for relative quantification in real-time RT-PCR. Nucleic Acids Researc. 2001;29:900-5.

[72] Liu H, Jiang Y, Luo Y, Jiang W. A simple and rapid determination of ATP, ADP and AMP concentrations in pericarp tissue of litchi fruit by high performance liquid chromatography. Food Technol Biotechnol. 2006.

[73] Suryawan A, Nguyen HV, Bush JA, Davis TA. Developmental changes in the feeding-induced activation of the insulin-signaling pathway in neonatal pigs. Am J Physiol Endocrinol Metab. 2001;281(5):E908.

[74] Bruce-Keller AJ, Salbaum JM, Luo M, Blanchard E, Taylor CM, Welsh DA, et al. Obese-type gut microbiota induce neurobehavioral changes in the absence of obesity. Biological Psychiatry. 2015;77(7):607-15.

[75] Hu L, Che L, Wu C, Curtasu MV, Wu F, Fang Z. Metabolomic profiling reveals the difference on reproductive performance between high and low lactational weight loss sows. Metabolomics. 2019;9:295.

[76] Chambers MC, Maclean B, Burke R, Amodei D, Ruderman DL, Neumann S, et al. A cross-platform toolkit for mass spectrometry and proteomics. Nat Biotechnol. 2012;30:918-20.

[77] Jia H, Shen X, Guan Y, Xu M, Tu J, Mo M, et al. Predicting the pathological response to neoadjuvant chemoradiation using untargeted metabolomics in locally advanced rectal cancer. Radiother Oncol. 2018;128(3):548-56.

[78] Wang H, Liu Z, Wang S, Cui D, Zhang X, Liu Y, et al. UHPLC-Q-TOF/MS based plasma metabolomics reveals the metabolic perturbations by manganese exposure in rat models. Metallomics. 2017;9(2):192-203.

[79] Feng JH, Wu HF, Chen Z. Metabolic responses of HeLa cells to silica nanoparticles by NMR-based metabolomic analyses. Metabolomics. 2013;9(4):874-86.

[80] Dervishi E, Zhang G, Dunn SM, Mandal R, Wishart DS, Ametaj BN. GC-MS Metabolomics identifies metabolite alterations that precede subclinical mastitis in the blood of transition dairy cows. J Proteome Res. 2016. doi: 10.1021/acs.jproteome.6b00538.

Tables

Table 1 Effects of maternal gut microbiota transplantation on the serum indicator of newborns in a piglet model[1]

Variable	CV	FMT	*P-value*
TC, mmol/L	2.00 ± 0.18	1.92 ± 0.1	0.68
TG, mmol/L	0.51 ± 0.05	0.39 ± 0.04	0.08
HDL, mmol/L	0.78 ± 0.06	0.89 ± 0.06	0.24
LDL, mmol/L	0.99 ± 0.12	1.12 ± 0.06	0.36
Glucose, mmol/L	5.32 ± 0.53	5.38 ± 0.22	0.91
Adiponectin, ug/L	81.51 ± 2.06 [a]	68.24 ± 2.28 [b]	<0.01
Glucagon, pg/ml	27.36 ± 0.75	26.54 ± 0.97	0.52
GLP-1, pmol/L	2.61 ± 0.08 [a]	2.16 ± 0.04 [b]	<0.01
Insulin, mIU/L	10.78 ± 0.35 [a]	8.98 ± 0.48 [b]	0.01
Leptin, ng/L	1351.69 ± 29.59	1302.30 ± 25.54	0.23

[1] Values are means ± SEMs, n = 6/group.

CV, Conventional pigs; FMT, healthy sow fecal microbiota were transplanted into newborn germ-free pigs; TC, total cholesterol; TG, triglyceride; HDL-c, high density lipoprotein-cholesterol; LDL-c, low density lipoprotein-cholesterol; GLP-1, Glucagon like peptide 1.

[a, b] Labeled means with different superscripts within a row are significantly different at $P < 0.05$.

Table 2 Effects of maternal gut microbiota transplantation on the lipid and glycogen contents, and enzymatic activities associated with lipids metabolism in liver and longissimus dorsi of newborns in a piglet model[1]

Variable	CV	FMT	*P-value*
Liver			
Lipid content, %	3.20 ± 0.25 [b]	4.20 ± 0.27 [a]	0.02
Glycogen (mg/g)	28.81 ± 4.76 [a]	14.29 ± 2.78 [b]	0.02
CPT-1 (ng/L)	233.91 ± 9.82 [a]	193.25 ± 11.61 [b]	0.02
LPL (U/mgprot)	0.82 ± 0.09	0.70 ± 0.04	0.26
HL (U/mgprot)	0.68 ± 0.08	0.72 ± 0.04	0.71
MDH (U/mgprot)	36.79 ± 1.52	39.09 ± 1.73	0.34
Longissimus dorsi			
Lipid content, %	3.63 ± 0.37	4.01 ± 0.18	0.38
Glycogen (mg/g)	9.31 ± 1.21	8.12 ± 1.50	0.55
CPT-1 (ng/L)	204.18 ± 6.26	207.16 ± 4.73	0.71
LPL (U/mgprot)	0.54 ± 0.06	0.56 ± 0.05	0.84
HL (U/mgprot)	0.47 ± 0.03	0.76 ± 0.20	0.19
MDH (U/mgprot)	5.36 ± 0.39	4.97 ± 0.45	0.53

[1] Values are means ± SEMs, n = 6/group.

CV, Conventional pigs; FMT, healthy sow fecal microbiota were transplanted into newborn germ-free pigs; CPT-1, carnitine palmitoyltransferase 1, LPL, lipoprotein lipase; HL, hepatic lipase; MDH, malate dehydrogenase.

[a, b] Labeled means with different superscripts within a row are significantly different at $P < 0.05$.

Table 3 Effects of maternal gut microbiota transplantation on the mRNA abundances for key factors associated with lipid metabolism in liver and longissimus dorsi of newborns in a piglet model[1]

Variable	CV	FMT	*P-value*
Liver			
ACC	1.00 ± 0.20 [b]	1.64 ± 0.14 [a]	0.02
FAS	1.00 ± 0.13 [b]	2.96 ± 0.65 [a]	0.01
CD36	1.00 ± 0.1 [b]	1.47 ± 0.13 [a]	0.02
LPL	1.00 ± 0.45	1.14 ± 0.52	0.84
SREBP-1C	1.00 ± 0.25	1.06 ± 0.22	0.87
PPKAA1	1.00 ± 0.14	1.26 ± 0.19	0.30
PPKAA2	1.00 ± 0.16	1.39 ± 0.12	0.08
CPT-1B	1.00 ± 0.12 [b]	2.05 ± 0.65 [a]	<0.01
PNPLA2	1.00 ± 0.16 [b]	2.34 ± 0.27 [a]	<0.01
PGC-1α	1.00 ± 0.23 [b]	4.01 ± 0.43 [a]	<0.01
Longissimus dorsi			
ACC	1.00 ± 0.05	1.26 ± 0.17	0.17
FAS	1.00 ± 0.04 [b]	2.52 ± 0.48 [a]	0.01
CD36	1.00 ± 0.13	1.07 ± 0.09	0.68
LPL	1.00 ± 0.10 [b]	1.90 ± 0.23 [a]	<0.01
SREBP-1C	1.00 ± 0.06	0.92 ± 0.18	0.69
PPKAA1	1.00 ± 0.11	1.15 ± 0.10	0.37
PPKAA2	1.00 ± 0.12 [b]	1.66 ± 0.16 [a]	<0.01
CPT-1B	1.00 ± 0.10	0.89 ± 0.05	0.36
PNPLA2	1.00 ± 0.11 [b]	1.53 ± 0.18 [a]	0.03
PGC-1α	1.00 ± 0.13	0.94 ± 0.12	0.66

[1] Values are means ± SEMs, n = 6/group.

CV, Conventional pigs; FMT, healthy sow fecal microbiota were transplanted into newborn germ-free pigs; ACC, acetyl-CoA carboxylase; FAS, fatty acid synthase; CD36, atty acid transporter CD36; LPL, lipoprotein lipase; SREBP-1C, sterol regulatory element binding protein 1C; PRKAA1, AMP activated alpha 1; PRKAA2,

AMP activated alpha 2; CPT-1B, carnitine palmitoyltransferase 1 B; PNPLA2, adipose triglyceride lipase; PGC-1α, peroxisome proliferator-activated receptor gamma coactivator-1α.

[a, b] Labeled means with different superscripts within a row are significantly different at $P < 0.05$.

Table 4 Effects of maternal gut microbiota transplantation on the mRNA abundances for key factors associated with glucose metabolism in liver and longissimus dorsi of newborns in a piglet model[1]

Variable	CV	FMT	*P-value*
Liver			
INSR	1.00 ± 0.09 [b]	1.77 ± 0.16 [a]	<0.01
INS1	1.00 ± 0.15 [b]	2.04 ± 0.32 [a]	0.02
PIK3	1.00 ± 0.16 [b]	1.84 ± 0.19 [a]	<0.01
SLC2a	1.00 ± 0.11	1.44 ± 0.22	0.12
GSK3	1.00 ± 0.10	1.39 ± 0.16	0.07
GYS2	1.00 ± 0.23 [b]	3.20 ± 0.46 [a]	<0.01
PCK1	1.00 ± 0.55 [b]	8.67 ± 1.44 [a]	<0.01
G6PC	1.00 ± 0.46 [b]	6.94 ± 1.81 [a]	0.01
Longissimus dorsi			
INSR	1.00 ± 0.04 [b]	1.38 ± 0.12 [a]	0.02
INS1	1.00 ± 0.14	1.10 ± 0.09	0.56
PIK3	1.00 ± 0.12	1.37 ± 0.11	0.06
SLC2a	1.00 ± 0.08	0.92 ± 0.11	0.57
GSK3	1.00 ± 0.10	1.07 ± 0.10	0.67
GYS2	1.00 ± 0.44	0.86 ± 0.17	0.77
PCK1	1.00 ± 0.33	1.26 ± 0.19	0.52

[1] Values are means ± SEMs, n = 6/group.

CV, Conventional pigs; FMT, healthy sow fecal microbiota were transplanted into newborn germ-free pigs; INSR, insulin receptor; IRS1, insulin receptor substrate 1; PIK3, phosphatidylinositol 3-kinase catalytic subunit type 3; SLC-2α, solute carrier family 2 member; G6PC, glucose-6-phosphatase; PCK 1, phosphoenolpyruvate carboxykinase 1; GSK 3, glycogen synthase kinase 3; GYS2, glycogen synthase 2.

[a, b] Labeled means with different superscripts within a row are significantly different at $P < 0.05$.

Table 5 Effects of maternal gut microbiota transplantation on the concentrations of adenosine in liver and longissimus dorsi of newborns in a piglet model[1]

Variable	CV	FMT	*P-value*
Liver			
ATP (ug/g)	19.91 ± 0.61 [b]	48.10 ± 1.22 [a]	<0.01
ADP (ug/g)	2169.6 ± 68.27 [a]	976.3 ± 30.72 [b]	<0.01
AMP (ug/g)	142.3 ± 9.23 [a]	79.71 ± 5.17 [b]	<0.01
AMP/ATP	7.17 ± 0.49 [a]	1.65 ± 0.09 [b]	<0.01
Longissimus dorsi			
ATP (ug/g)	280.0 ± 42.55 [a]	167.8 ± 14.31 [b]	0.03
ADP (ug/g)	547.6 ± 98.67 [a]	190.0 ± 10.65 [b]	<0.01
AMP (ug/g)	145.5 ± 19.57 [a]	82.53 ± 7.41 [b]	0.02
AMP/ATP	0.53 ± 0.02	0.59 ± 0.08	0.68

[1] Values are means ± SEMs, n = 6/group.

CV, Conventional pigs; FMT, healthy sow fecal microbiota were transplanted into newborn germ-free pigs; ATP, adenosine triphosphate; ADP, adenosine diphosphate; AMP, adenosine monophosphate.

[a, b] Labeled means with different superscripts within a row are significantly different at $P < 0.05$.

Figures

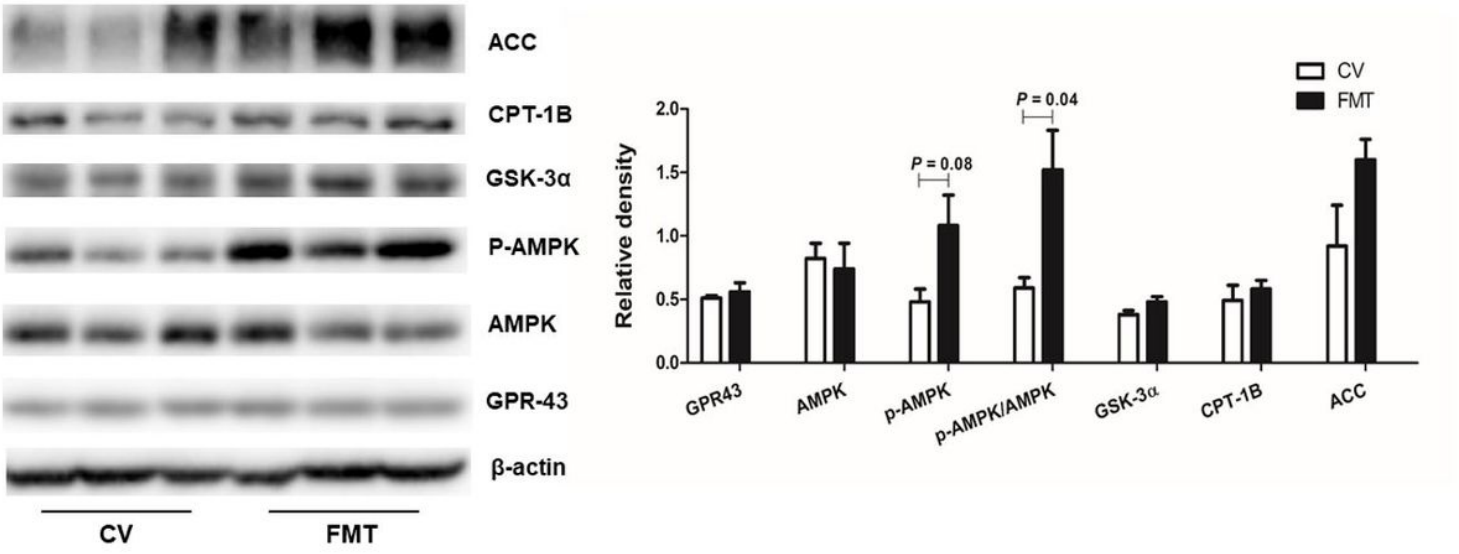

Figure 1

Effect of maternal gut microbiota transplantation on the protein levels of GPR43, p-AMPK, T-AMPK, CPT-1B, GSK3-α, ACC in liver of newborns in a piglet model. CV, Conventional pigs; FMT, healthy sow fecal microbiota were transplanted into newborn germ-free pigs; ACC, acetyl-CoA carboxylase; CPT-1B, carnitine palmitoyltransferase 1 B; p-AMPK, phosphorylated adenosine monophosphate-activated protein kinase; AMPK, adenosine monophosphate-activated protein kinase; GPR43, G-protein-coupled receptors 43.

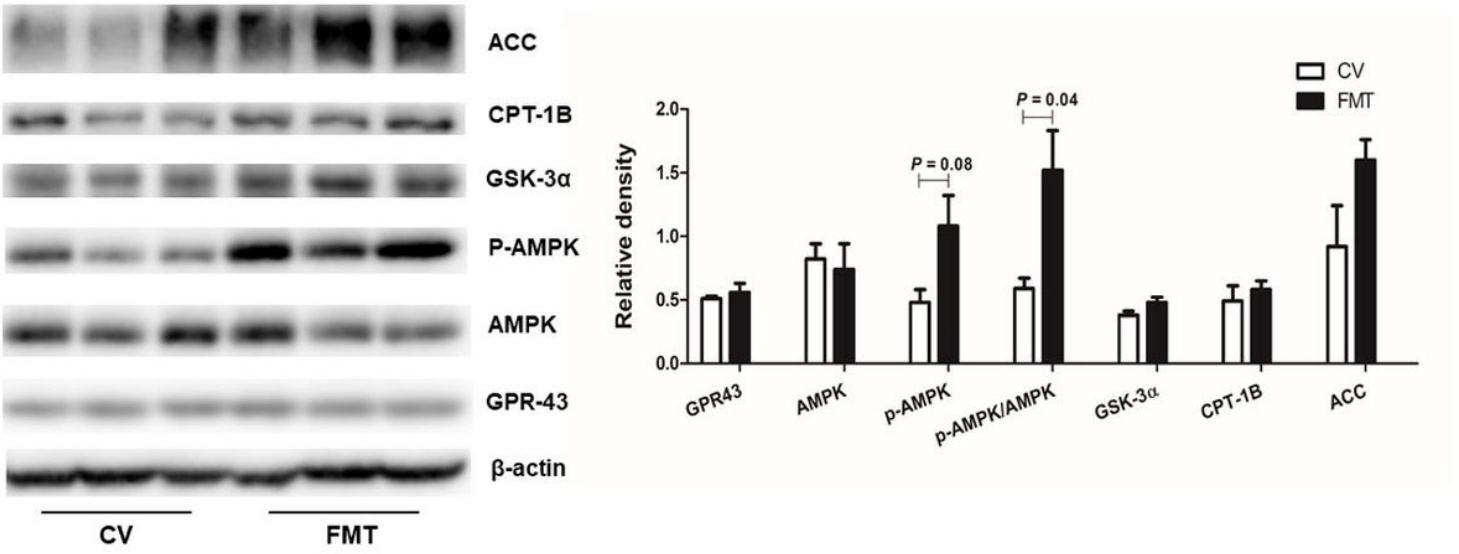

Figure 1

Effect of maternal gut microbiota transplantation on the protein levels of GPR43, p-AMPK, T-AMPK, CPT-1B, GSK3-α, ACC in liver of newborns in a piglet model. CV, Conventional pigs; FMT, healthy sow fecal

microbiota were transplanted into newborn germ-free pigs; ACC, acetyl-CoA carboxylase; CPT-1B, carnitine palmitoyltransferase 1 B; p-AMPK, phosphorylated adenosine monophosphate-activated protein kinase; AMPK, adenosine monophosphate-activated protein kinase; GPR43, G-protein-coupled receptors 43.

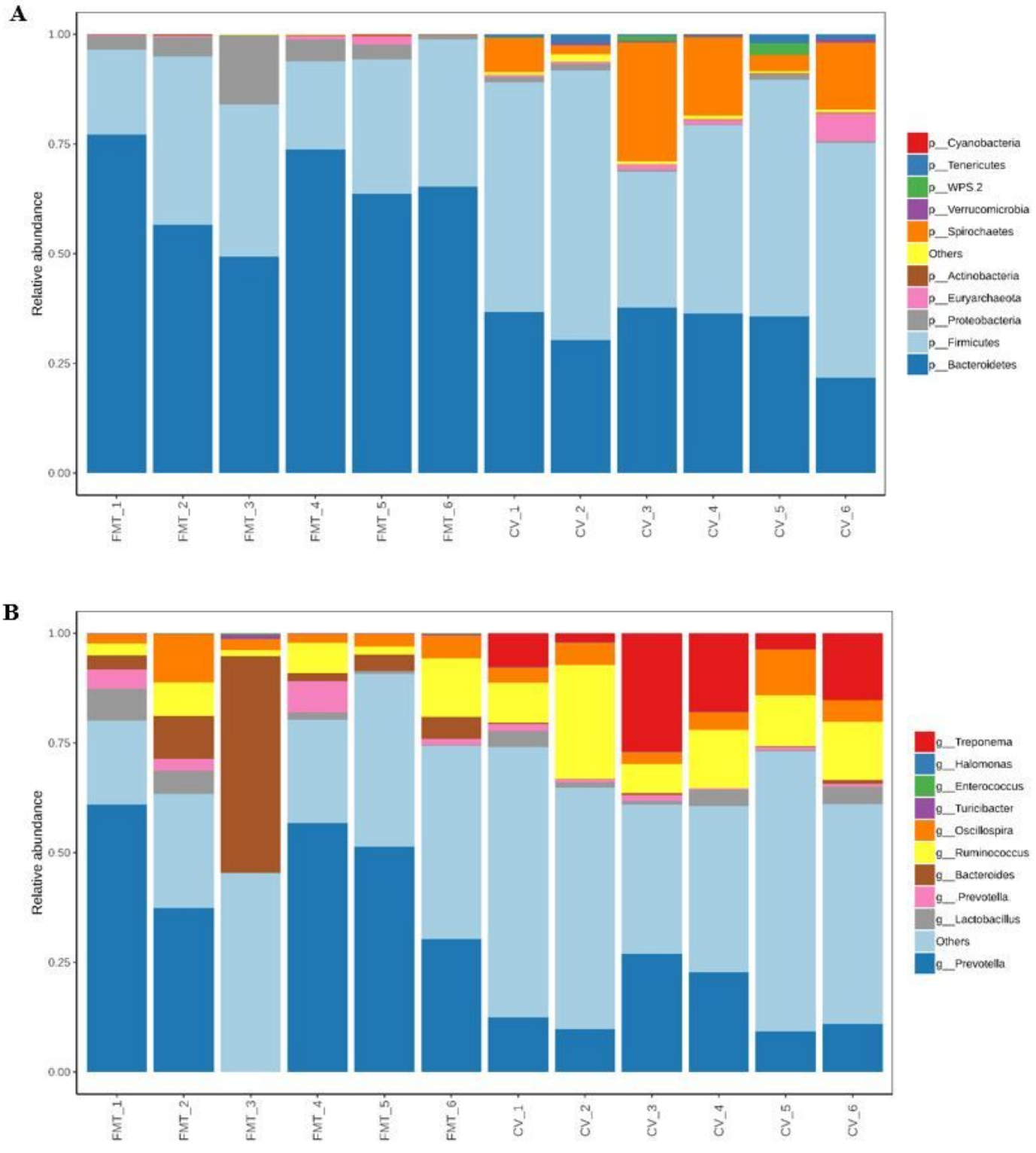

Figure 2

16S rRNA gene analysis reveals phyla, order and genus level differences in colonic microbiota of FMT and CV pigs. Relative abundance levels of the bacterial phyla present in FMT and CV pigs (A). Relative

abundance levels of the bacterial genus present in FMT and CV pigs (B). CV, Conventional pigs; FMT, healthy sow fecal microbiota were transplanted into newborn germ-free pigs.

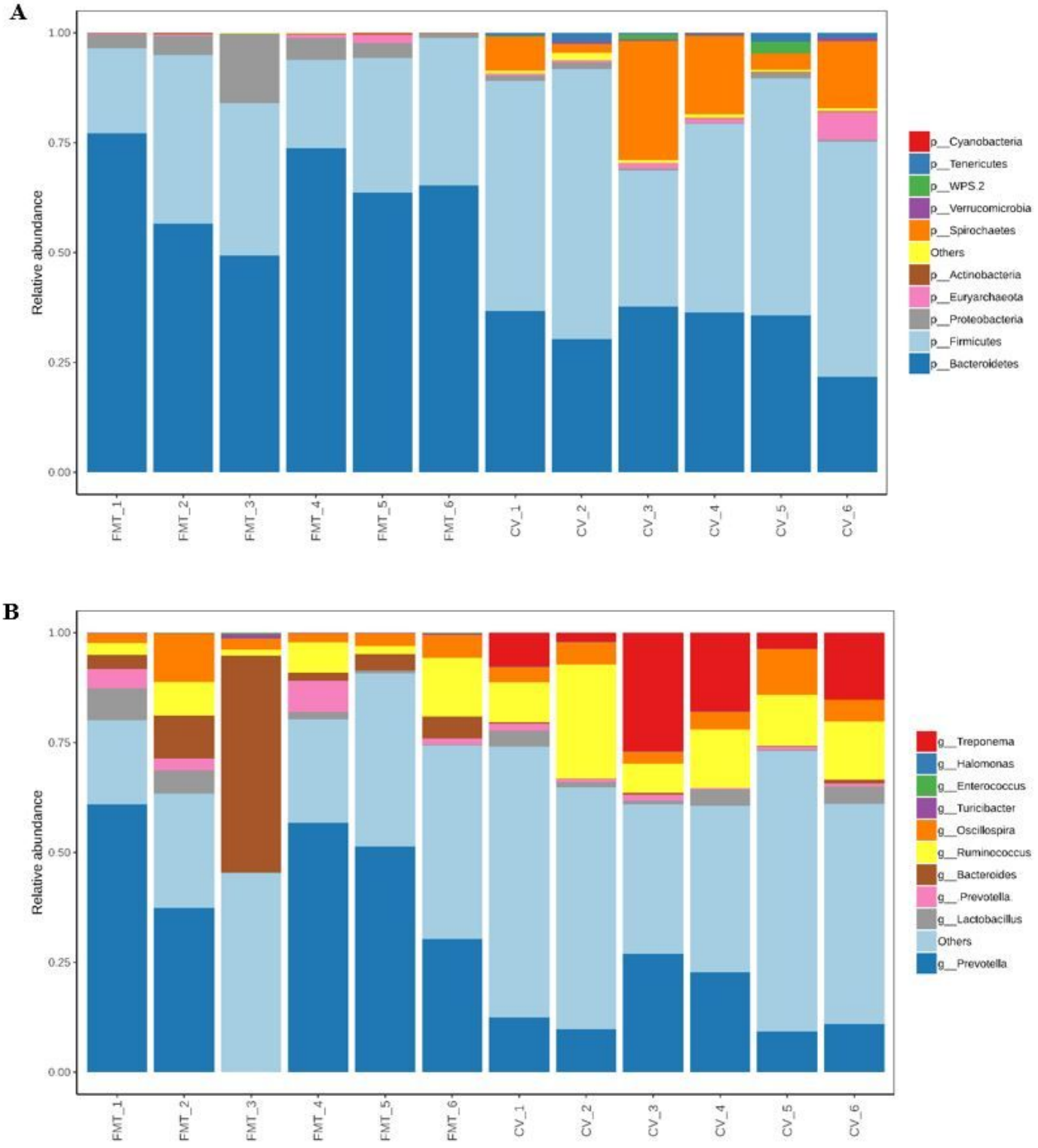

Figure 2

16S rRNA gene analysis reveals phyla, order and genus level differences in colonic microbiota of FMT and CV pigs. Relative abundance levels of the bacterial phyla present in FMT and CV pigs (A). Relative

abundance levels of the bacterial genus present in FMT and CV pigs (B). CV, Conventional pigs; FMT, healthy sow fecal microbiota were transplanted into newborn germ-free pigs.

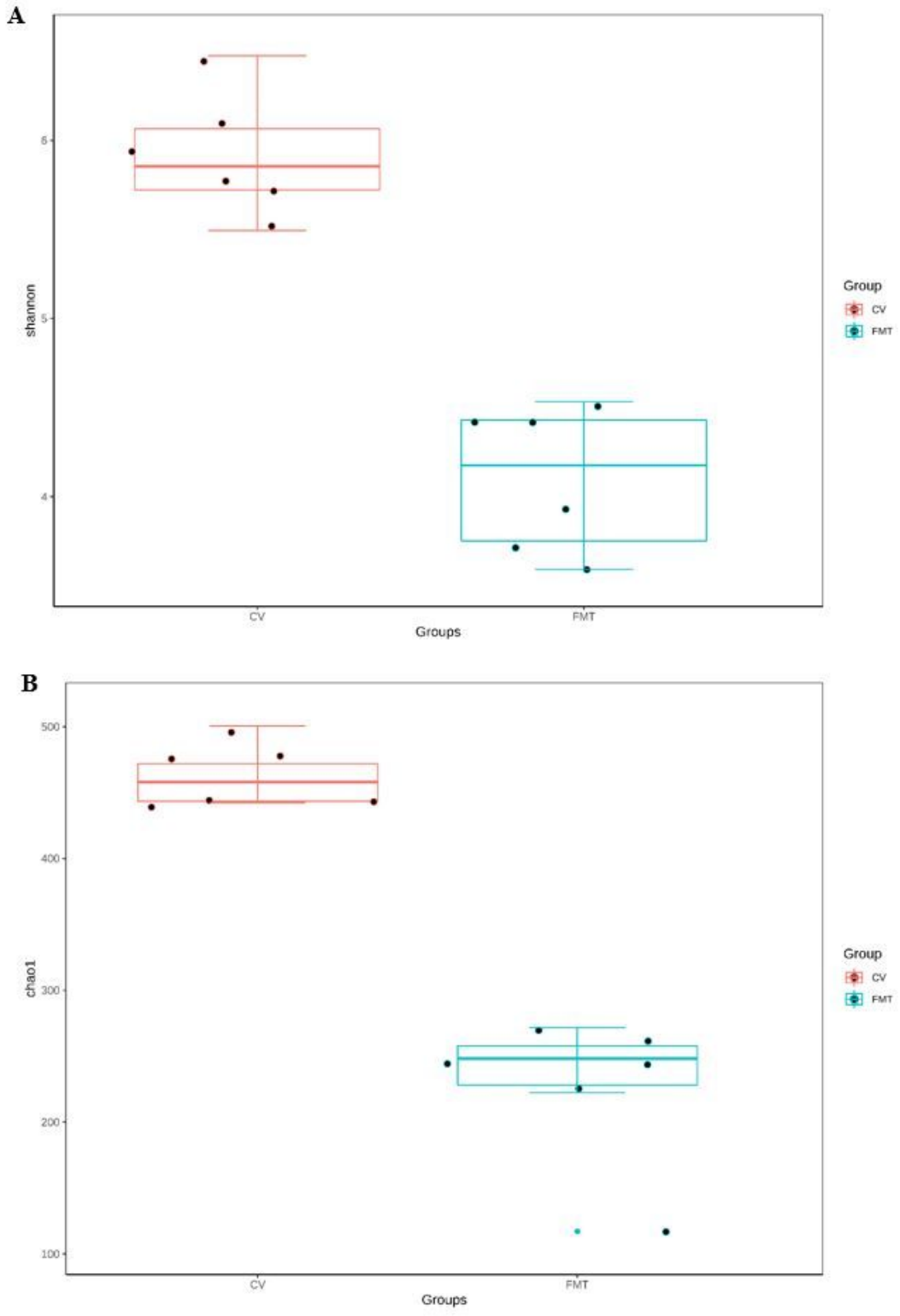

Figure 3

Alpha diversity index of colonic microflora in FMT and CV pigs. The Shannon index (A) and Chao1 index (B) of colonic microflora in FMT and CV pigs. CV, Conventional pigs; FMT, healthy sow fecal microbiota were transplanted into newborn germ-free pigs.

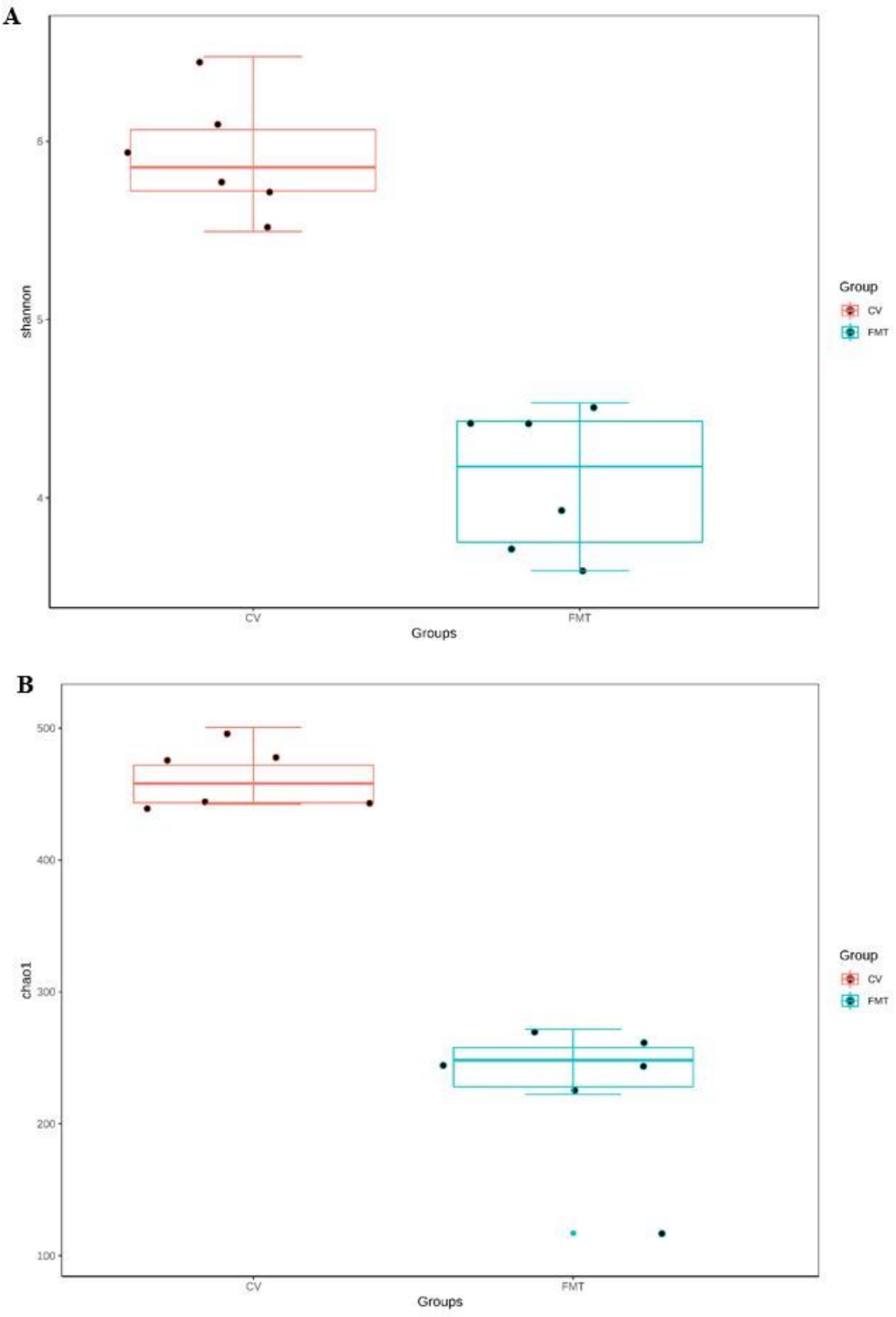

Figure 3

Alpha diversity index of colonic microflora in FMT and CV pigs. The Shannon index (A) and Chao1 index (B) of colonic microflora in FMT and CV pigs. CV, Conventional pigs; FMT, healthy sow fecal microbiota were transplanted into newborn germ-free pigs.

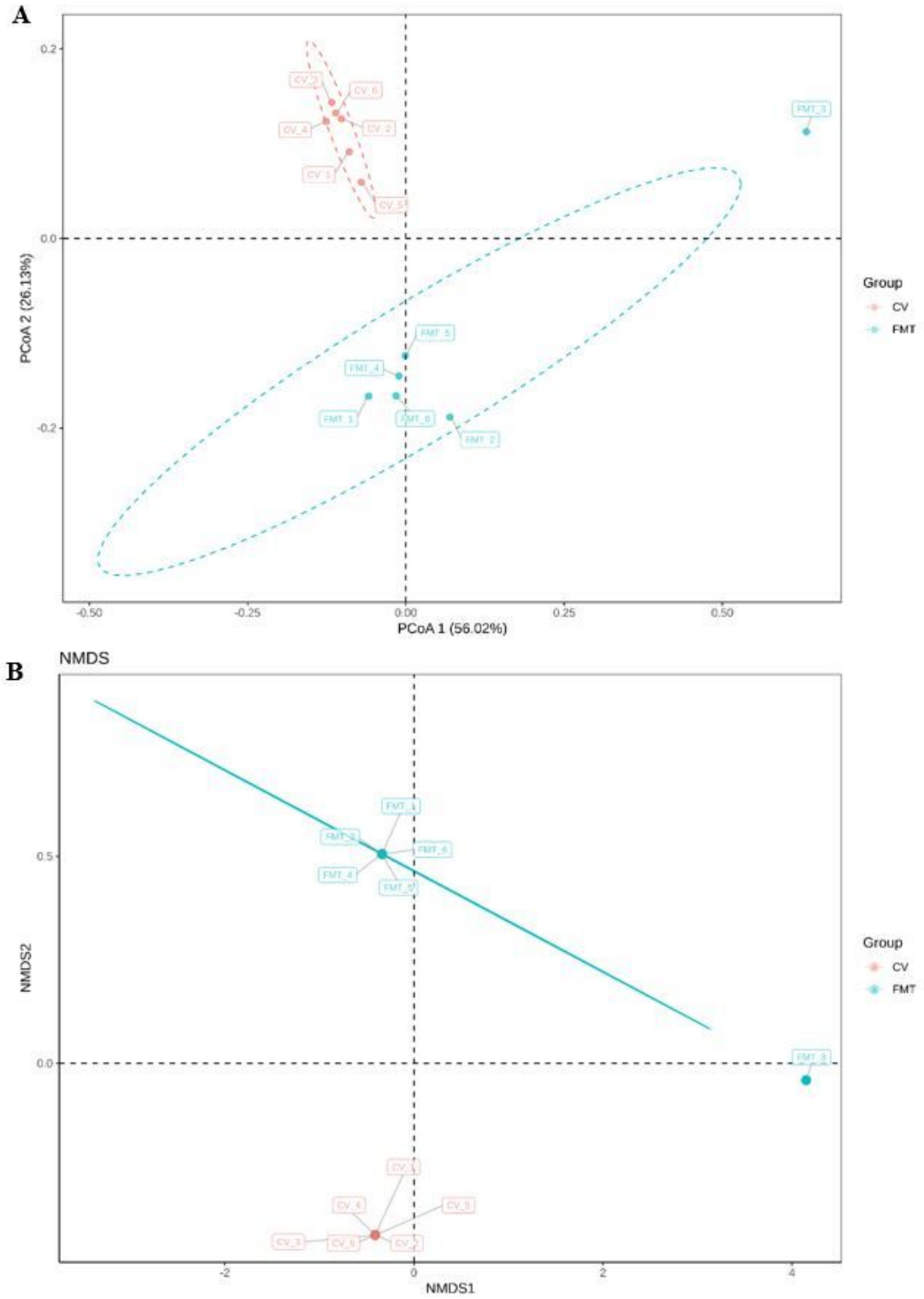

Figure 4

Principal co-ordinates analysis to visualize the Euclidean distances (A) and Non-metric multi-dimensional scaling analysis to visualize the Bray-Curtis distances (B) of colonic microflora in FMT and CV pigs. CV, Conventional pigs; FMT, healthy sow fecal microbiota were transplanted into newborn germ-free pigs.

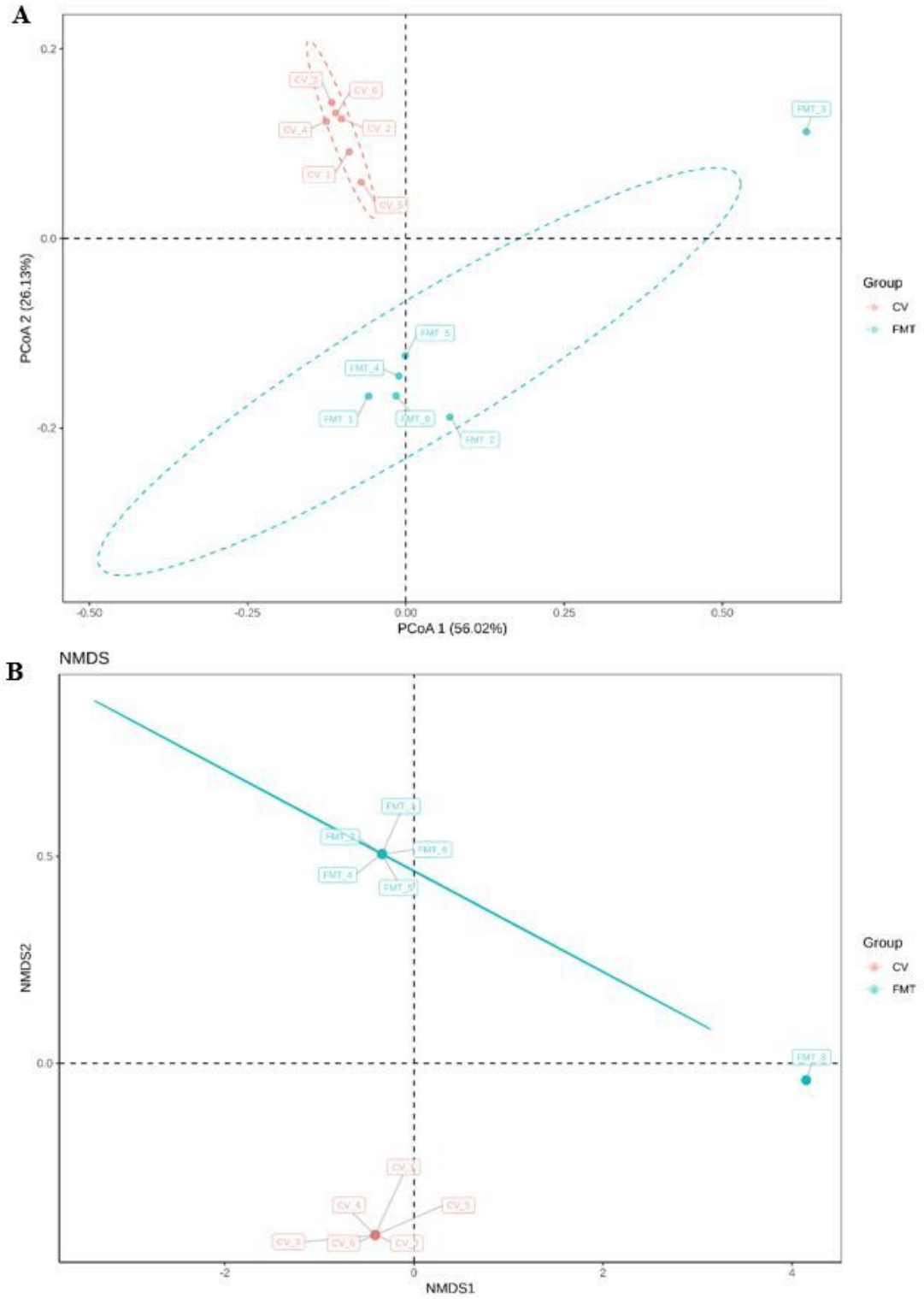

Figure 4

Principal co-ordinates analysis to visualize the Euclidean distances (A) and Non-metric multi-dimensional scaling analysis to visualize the Bray-Curtis distances (B) of colonic microflora in FMT and CV pigs. CV, Conventional pigs; FMT, healthy sow fecal microbiota were transplanted into newborn germ-free pigs.

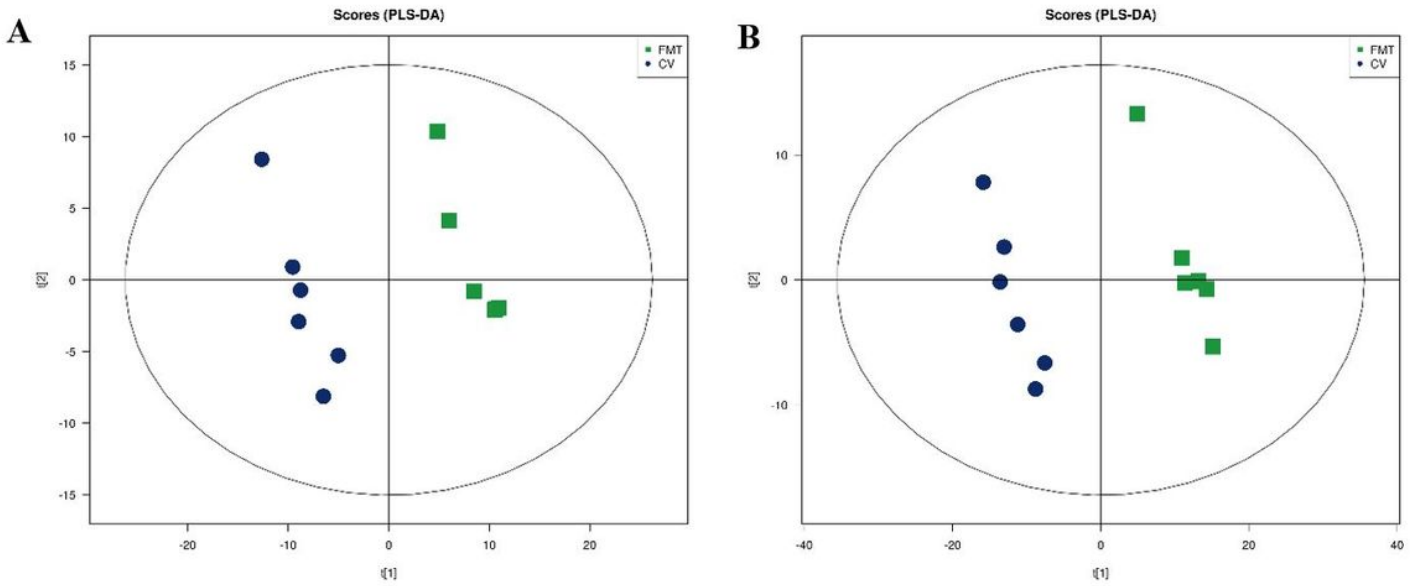

Figure 5

PLS-DA score map derived from UHPLC-Q-TOF/MS spectra concerning FMT (blue rotundities) and CV (green squares) serum of pigs in the positive mode (R2X = 0.336, R2Y = 0.99, Q2 = 0.782; (A)) and negative mode (R2X = 0.477, R2Y = 0.994, Q2 = 0.936; (B)). PLS-DA, Partial least squares discriminant; CV, Conventional pigs; FMT, healthy sow fecal microbiota were transplanted into newborn germ-free pigs.

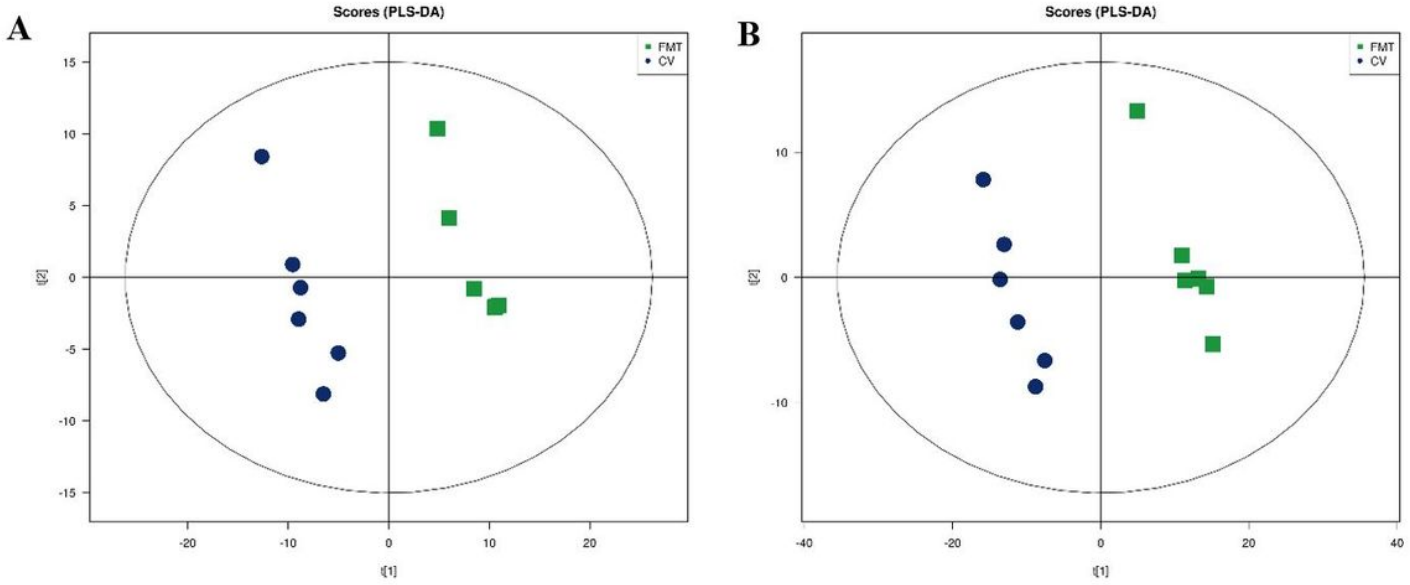

Figure 5

PLS-DA score map derived from UHPLC-Q-TOF/MS spectra concerning FMT (blue rotundities) and CV (green squares) serum of pigs in the positive mode (R2X = 0.336, R2Y = 0.99, Q2 = 0.782; (A)) and negative mode (R2X = 0.477, R2Y = 0.994, Q2 = 0.936; (B)). PLS-DA, Partial least squares discriminant; CV, Conventional pigs; FMT, healthy sow fecal microbiota were transplanted into newborn germ-free pigs.

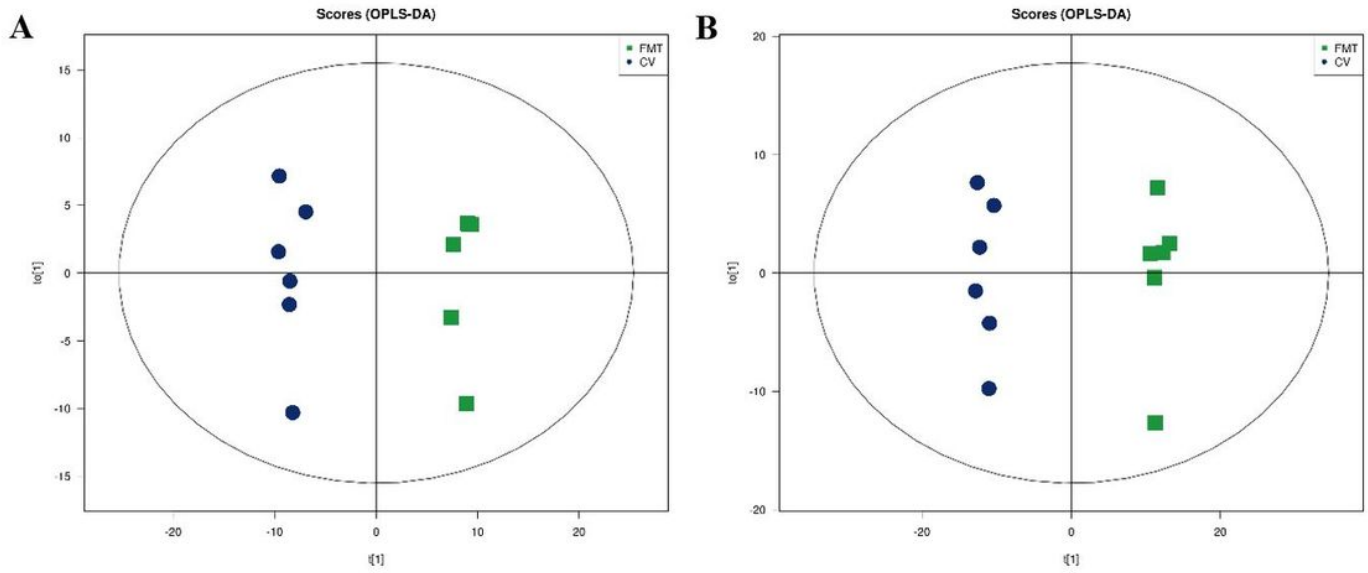

Figure 6

OPLS-DA score map derived from UHPLC-Q-TOF/MS spectra concerning GF (blue circles) and FA (green squares) serum of pigs in the positive mode (R2X = 0.336, R2Y = 0.99, Q2 = 0.824; (A)) and negative mode (R2X = 0.477, R2Y = 0.994, Q2 = 0.915; (B)) OPLS-DA, orthogonal partial least-squares discriminant. CV, Conventional pigs; FMT, healthy sow fecal microbiota were transplanted into newborn germ-free pigs.

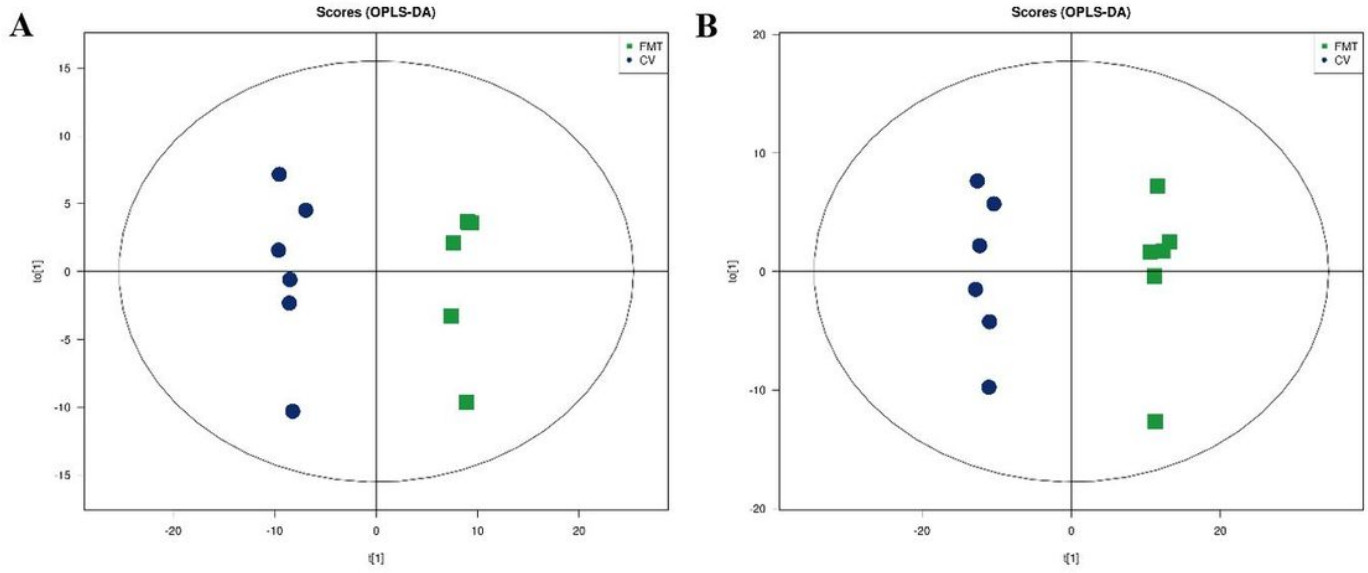

Figure 6

OPLS-DA score map derived from UHPLC-Q-TOF/MS spectra concerning GF (blue circles) and FA (green squares) serum of pigs in the positive mode (R2X = 0.336, R2Y = 0.99, Q2 = 0.824; (A)) and negative mode (R2X = 0.477, R2Y = 0.994, Q2 = 0.915; (B)) OPLS-DA, orthogonal partial least-squares discriminant. CV, Conventional pigs; FMT, healthy sow fecal microbiota were transplanted into newborn germ-free pigs.

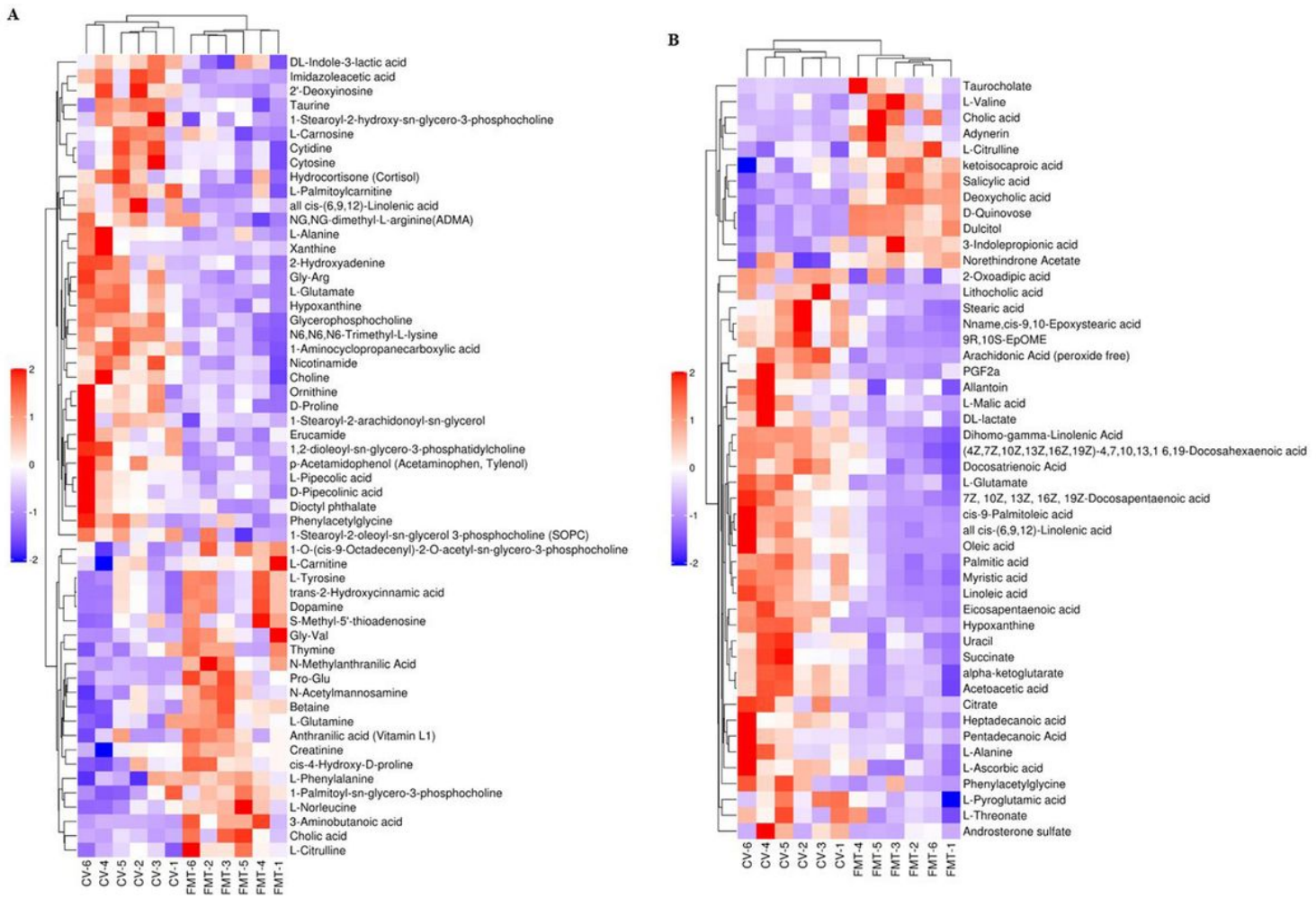

Figure 7

Hierarchical clustering heat map of significantly different metabolites from serum of pig in the positive mode (A) and negative mode (B). Metabolites peak area were Z score transformed. Warm color and cold color indicate increased and decreased expression of the metabolites, respectively. CV, Conventional pigs; FMT, healthy sow fecal microbiota were transplanted into newborn germ-free pigs.

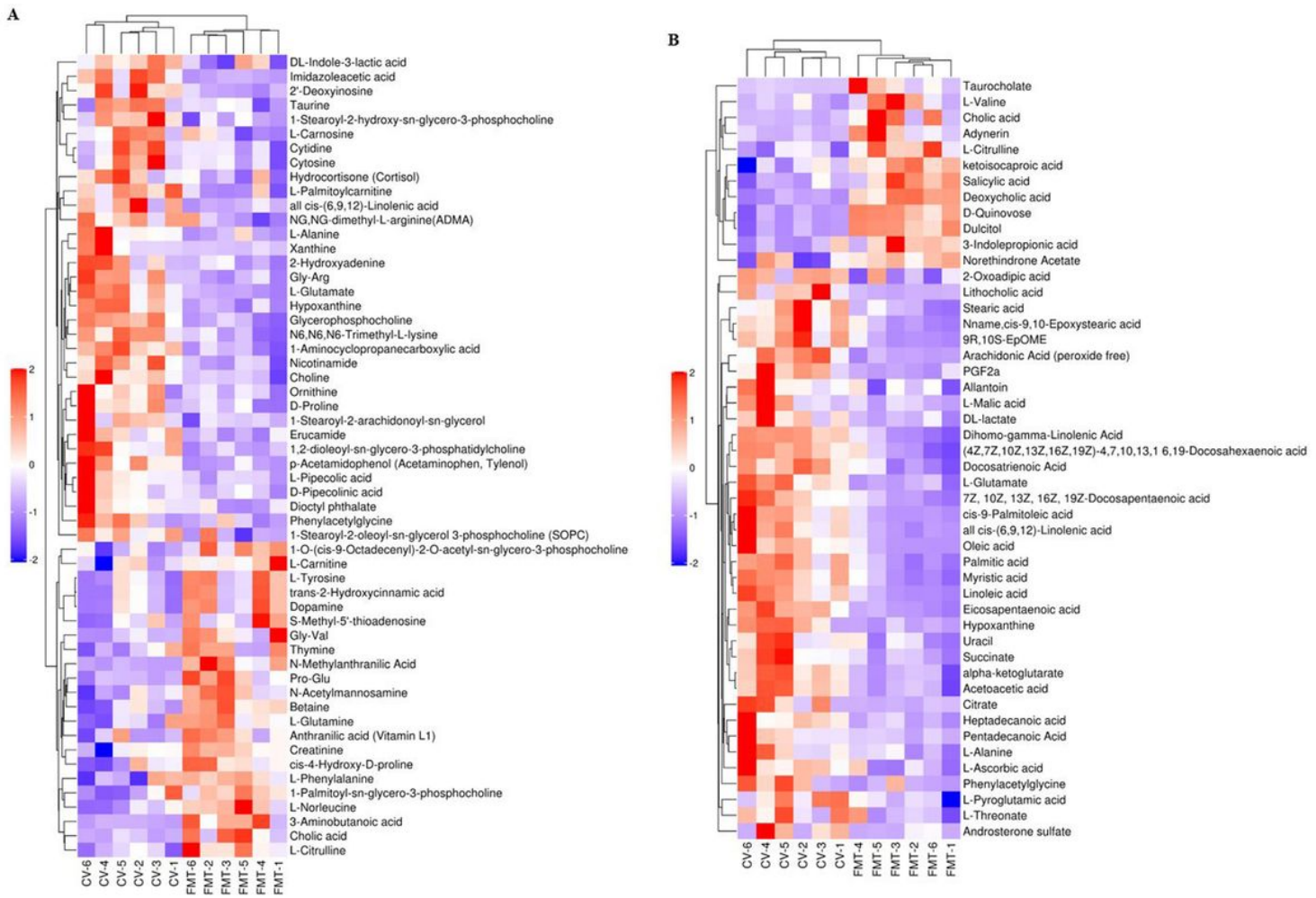

Figure 7

Hierarchical clustering heat map of significantly different metabolites from serum of pig in the positive mode (A) and negative mode (B). Metabolites peak area were Z score transformed. Warm color and cold color indicate increased and decreased expression of the metabolites, respectively. CV, Conventional pigs; FMT, healthy sow fecal microbiota were transplanted into newborn germ-free pigs.

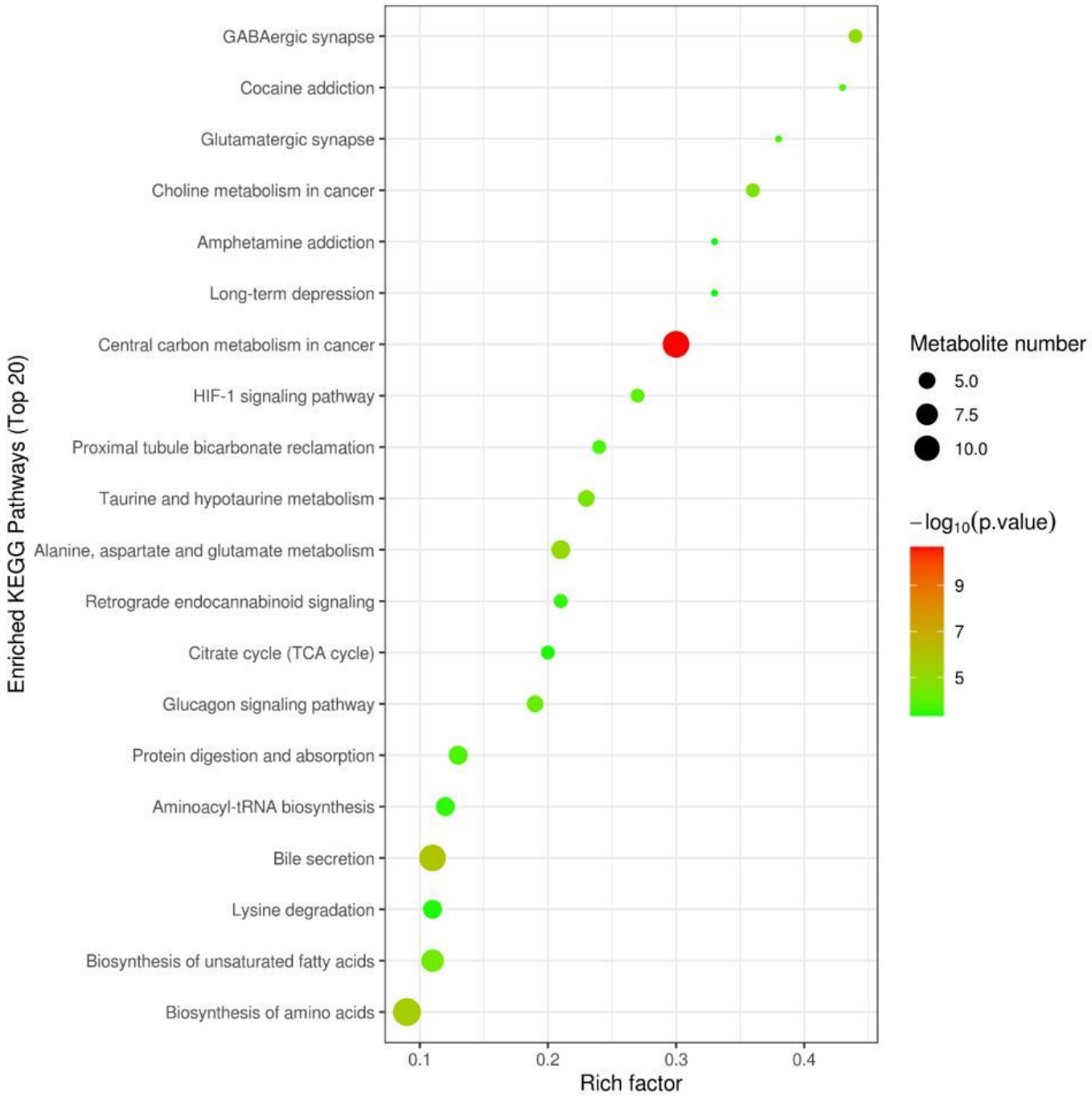

Figure 8

Topology analysis of metabolic pathways identified between GF and FA pigs. The X-axis represents the rich factor, and the Y-axis represents the pathway. Larger sizes and darker colors represent greater pathway enrichment and higher pathway impact values, respectively. CV, Conventional pigs; FMT, healthy sow fecal microbiota were transplanted into newborn germ-free pigs.

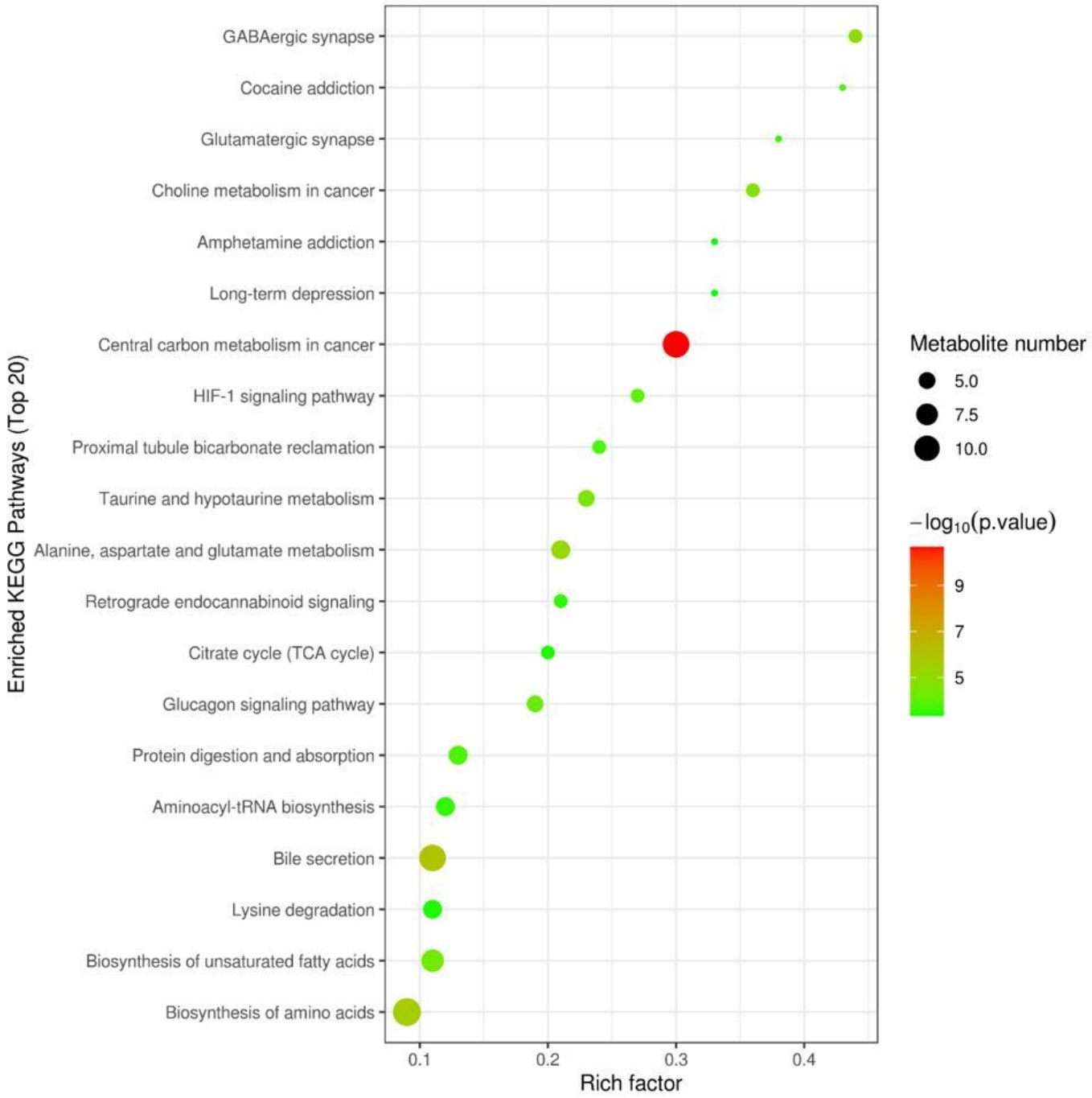

Figure 8

Topology analysis of metabolic pathways identified between GF and FA pigs. The X-axis represents the rich factor, and the Y-axis represents the pathway. Larger sizes and darker colors represent greater pathway enrichment and higher pathway impact values, respectively. CV, Conventional pigs; FMT, healthy sow fecal microbiota were transplanted into newborn germ-free pigs.

Supplementary Files

This is a list of supplementary files associated with this preprint. Click to download.

- 4SupplementarymaterialGN.docx
- 4SupplementarymaterialGN.docx